UNIVERSITY OF CALIFORNIA SAN DIEGO

Design and Material Characterization of an Inflatable Vaginal Dilator

A thesis submitted in partial satisfaction of the requirements
for the degree of Master of Science

in

Engineering Sciences (Mechanical Engineering)

by

Po-Han Chen

Committee in charge:

Professor Frank E. Talke, Chair
Professor Shengqiang Cai
Professor James R. Friend
Professor Milan Theodore Makale

2022

The thesis of Po-Han Chen is approved, and it is acceptable in quality and form for publication on microfilm and electronically.

University of California San Diego

2022

TABLE OF CONTENTS

LIST OF FIGURES

ACKNOWLEDGEMENTS

I want to start this acknowledgment by expressing my gratitude to Professor Frank Talke for leading me into his lab. He has been supporting and guiding me and the project with all his effort. With Professor Talke's encouragement, both the project and I have seen significant improvement.

I also want to express my gratitude to Dr. Jyoti Mayadev, Dr. Milan Makale, and Dr. Casey Williamson for all the support and advice. Because of their suggestions and knowledge, the new dilator prototype has been implemented successfully.

I would like to thank Dr. Karcher Morris for his help and willingness to teach me many useful skills. Without his support, I would not have been able to finish the experiments and the finite element analysis simulation. I would also like to thank Matthew Kohanfars for sharing not only a lot of design ideas for the dilator prototype but also putting a lot of effort into improving the design of the dilator.

Moreover, I want to express my appreciation to the members of the vaginal stenosis project, Brian Li, Rafaela Simoes-torigoe, and Shengfan Hu. I am thankful for all their assistance and collaboration with the data collection, design iterations, prototyping, and for making the project grow and advance. I would also like to thank Raphaelle Paracuellos and Gabrielle Scott for helping with correcting and proofreading my thesis and helping with the manufacturing issues and improving the dilator prototype.

Thank you to all the members in the Talke Lab for creating such a nice research environment. It was really great to work with everyone, and I really learned a lot from everyone's knowledge. Lastly, thank you to my family with for all their support.

Chapter 2 and Chapter 4, in part, contains published material as it appears in Rafaela Simoes-Torigoe, Po-Han Chen, Yu M. Li, Matthew Kohanfars, Karcher Morris, Casey W. Williamson, Milan Makale, Jyoti Mayadev, Frank Talke, "Design and Validation of an Automated Dilator Prototype for the Treatment of Radiation Induced Vaginal Injury," 2021 43rd Annual International Conference of the IEEE Engineering in Medicine & Biology Society (EMBC), IEEE. The thesis author was a co-author of this paper.

Chapter 2, in part, contains unpublished material as it appears in Shengfan Hu, Karcher Morris, Po-Han Chen, Rafaela Simoes-Torigoe, Yu M. Li, Milan Makale, Jyoti Mayadev, Frank Talke, "A Soft Robotic Closed-Loop System for the Treatment of Vaginal Stenosis," 2022 JSME-IIP/ASME-ISPS Joint International Conference on Micromechatronics for Information and Precision Equipment (MIPE2022). The thesis author was a co-author of this paper.

ABSTRACT OF THE THESIS

Design and Material Characterization of an Inflatable Vaginal Dilator

By

Po-Han Chen

Master of Science in Engineering Sciences (Mechanical Engineering)

University of California San Diego, 2022

Professor Frank E. Talke, Chair

Cervical cancer is a common malignancy worldwide and is one of the leading causes of death for women. Vaginal stenosis is a common long-term side effect of pelvic radiation. Vaginal dilator therapy is the most common and universally accepted strategy to prevent vaginal stenosis, as it can promote epithelialization and increased vascularity of the tissues after brachytherapy. However, many patients feel uncomfortable with using commercial vaginal dilators that are manufactured using hard latex materials, struggle with transitioning from one dilator size to another, and have difficulty dilating the apex of the vaginal canal. In this thesis, an inflatable vaginal dilator made from silicone polymers was developed to overcome the problems inherent with hard plastic dilators. Silicone polymers are soft and inflatable materials and ideally suited for this application. In this thesis, we have investigated the stress-strain characteristics of silicone material used for manufacturing vaginal dilators. We have determined a two-term Mooney-Rivlin

equation to describe the behavior of silicone. Finite element analysis was used to simulate the dilator inflation and determine the force that the dilator exerts on the vaginal wall. In addition, experimental studies were conducted to verify the finite element simulation. Silicone dilator balloons of various wall thicknesses were fabricated.

Chapter 1 Introduction

1.1 Medical Background

Cervical cancer is the fourth most common female malignancy worldwide, and is one of the leading causes of death for women [1] [2]. More than 500,000 women are diagnosed with cervical cancer each year and over 300,000 deaths occur per year [1]. Figure 1 shows the cervical cancer incidence ranking compared to other cancers in the world. In 2018, twenty-eight countries were identified to have cervical cancer as the highest cancer rate in their country globally, with highest incidence countries concentrated in Africa [3]. With this surprising number of patients suffering from this disease, it is important to consider both the treatment efficacy for cervical cancer, but also the issues that arise following treatment to help women recovering from radiation-induced injury.

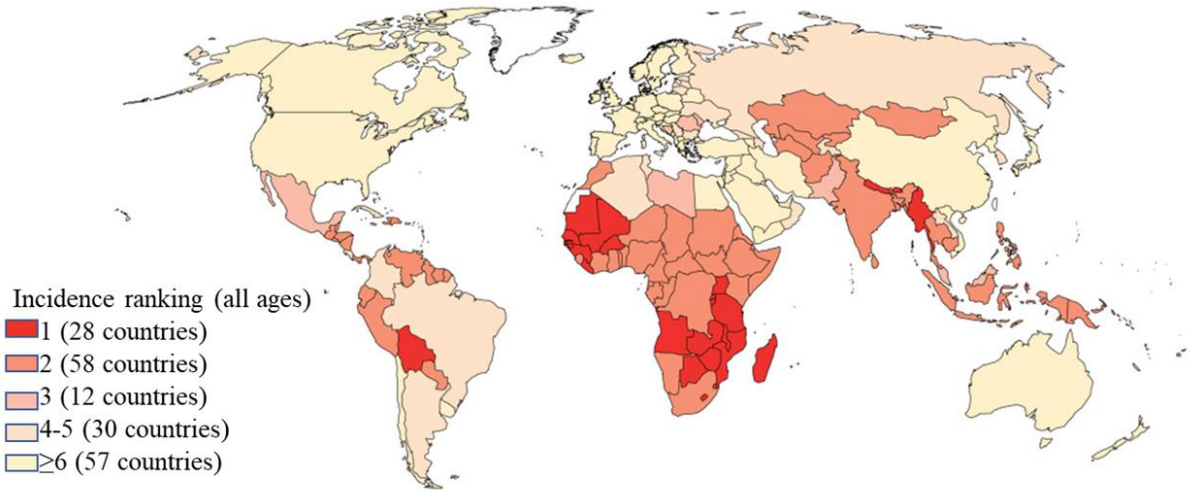

Figure 1: Incidence ranking of cervical cancer compared to other cancer in 2018 of all ages women [3]

1.1.1 Radiotherapy in Treating Cervical Cancer

The treatment of cervical cancer can include surgery, radiation, and chemotherapy [4]. The most common treatments for cervical cancer are pelvic radiation therapy (RT) and brachytherapy [5]. Brachytherapy is a type of radiation therapy where the doctor inserts a radioactive material inside a localized portion of the body to treat cancer. This is also referred to as internal radiation, while pelvic radiation therapy projects radiation from an external radiation source [6].

1.1.2 Effect of Radiation Therapy and Radiation on Tissue

Adverse events for both pelvic radiation therapy and brachytherapy can be divided into short-term and long-term side effects. Some common short-term side effects include tiredness, upset stomach, loose stools, nausea, and vomiting [7]. In addition, radiation can also irritate the vagina, causing radiation vaginitis [7]. The most common long-term side effects are lymphedema, premature menopause, and vaginal stenosis (VS) [7]. Vaginal stenosis is characterized by the buildup of scar tissue in the vaginal canal, which causes the vagina to become shorter, narrower, less flexible, drier, and more fragile. It can also result in dyspareunia and a reduced ability of doctors to conduct pelvic examinations [8]. This thesis will focus on the design of a vaginal dilator used for the treatment of long-term radiation injury of cervical tissue.

Through an examination of vaginal biopsies after radiotherapy, it was found that chronic effects of radiation included tissue atrophy, formation of scar tissue, and vasculature changes [9].

Figure 2 illustrates the difference between the vaginal wall before and after radiation. We observe that after the radiation of tissue, epithelial denudation occurs. These changes will cause loss of elasticity of the vaginal tissue and stenosis of the vaginal canal.

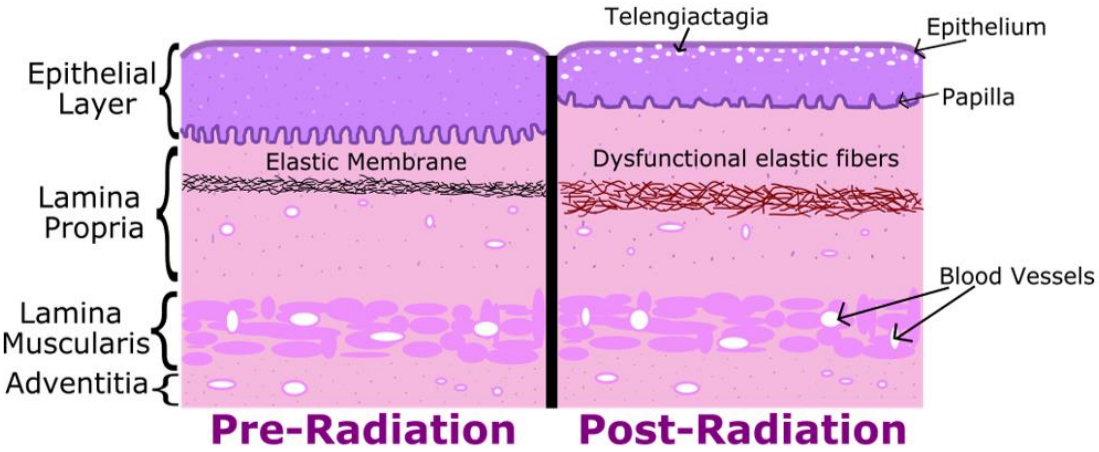

Figure 2: Tissue effect of radiation [50]

1.1.3 Current Treatment of Vaginal Stenosis After Radiation

Since vaginal stenosis occurs from either pelvic radiation therapy or brachytherapy, there are several treatments to prevent or reduce the severity of vaginal stenosis in cervical cancer patients. These include vaginal dilator therapy, hyaluronic acid therapy, intravaginal laser therapy, and vaginal estrogen therapy [10]. Among the aforementioned treatment methods, vaginal dilator therapy is the globally accepted vaginal stenosis prevention strategy [10].

1.1.3.1 Vaginal Dilators

Vaginal dilators are often prescribed by doctors to decrease anxiety and pain in anticipation of dyspareunia (genital pain during intercourse) or vaginal examinations [11]. The use of vaginal dilators can promote epithelialization and increased vascularity of the tissues after radiation treatment [12]. Vaginal dilators are typically smooth, cylindrical devices that are inserted into a woman's vagina to facilitate the stretching and relaxation of the underlying tissues [11]. These vaginal dilators are commonly sold in multiple sizes [13] as shown in Figure 3. They are typically made of hard plastic or latex materials. Some dilator models have additional features to improve user experiences, such as temperature or vibration control. For instance, dilators that feature an auto-heated, vibrating design help decrease pain sensitivity and dilator handles make it easier to insert and hold the dilator in place [11].

Figure 3: Commercially available vaginal dilators

1.1.3.2 Potential Problems with Vaginal Dilators

Often, patients undergoing dilator therapy experience issues when transitioning from one dilator to the next larger size, or they can even find the insertion of the smallest size very painful [18]. Since the sizes of commercially available dilators are fixed, patients who cannot transition to the next size frequently give up on this treatment altogether. Additionally, the rigidity of the dilators can cause pain and extreme discomfort for patients. Vaginal dilator therapy often requires weeks or months to be successful, and treatment can become expensive, time-consuming, and physically painful [14].

1.1.4 Need for an Inflatable Balloon Dilator

As a result of these difficulties in vaginal stenosis therapy, patient adherence to long term dilator therapy is low (Figure 4) [15]. A soft, inflatable dilator design would be highly desirable, especially if it could address the issue of size and rigidity and reduce pain during treatment for vaginal stenosis. Such a design could also incorporate a monitoring system to provide real-time feedback on the inflation of the dilator, allowing patients to determine what size dilator is most comfortable for them during therapy.

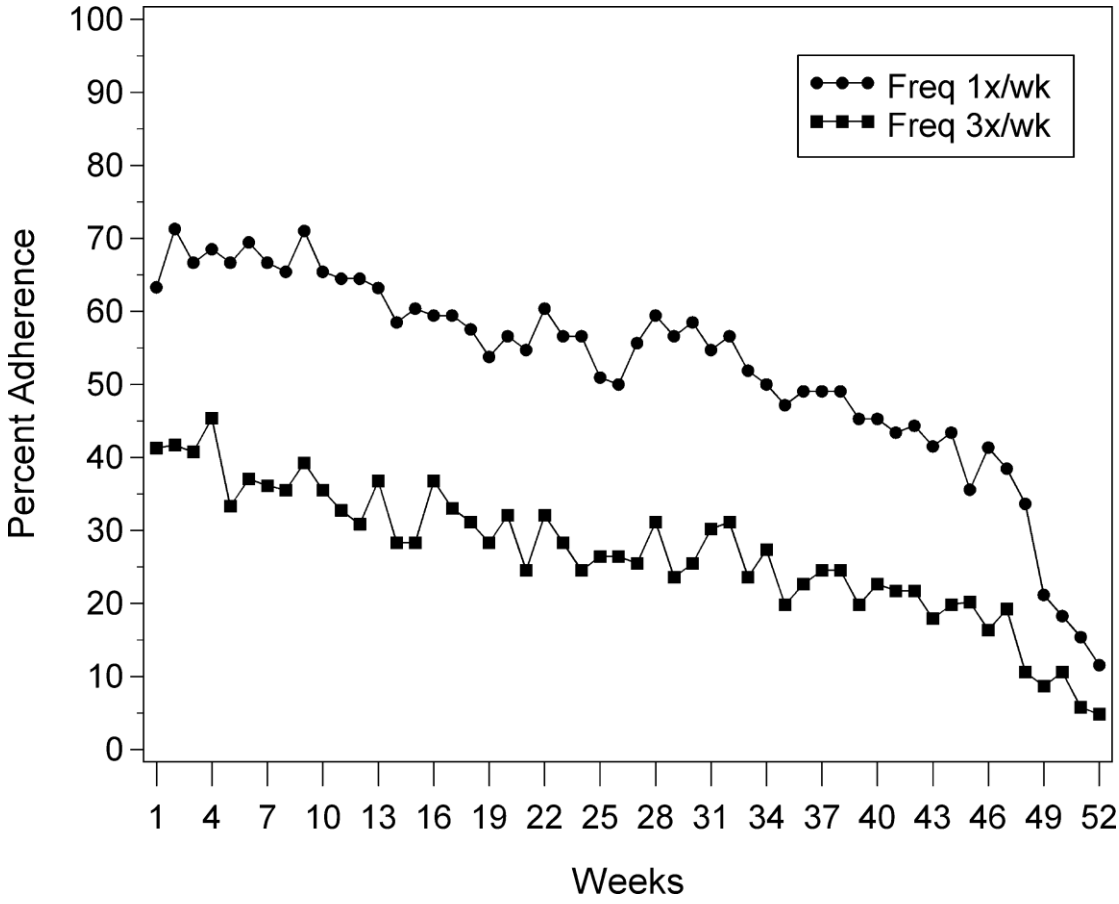

Figure 4: Patient adherence of vaginal dilator for 3 times a week and once a week [15]

1.1.4.1 Materials for Dilator

Commercially available silicone materials were investigated as candidates for dilator materials and found to be a good choice for inflatable dilators. Figure 5 shows the Shore hardness scale of typical polymers [16]. The materials used for the manufacturing of inflatable dilators were based on silicone of Shore hardness A10 (Dragon Skin 10 medium).

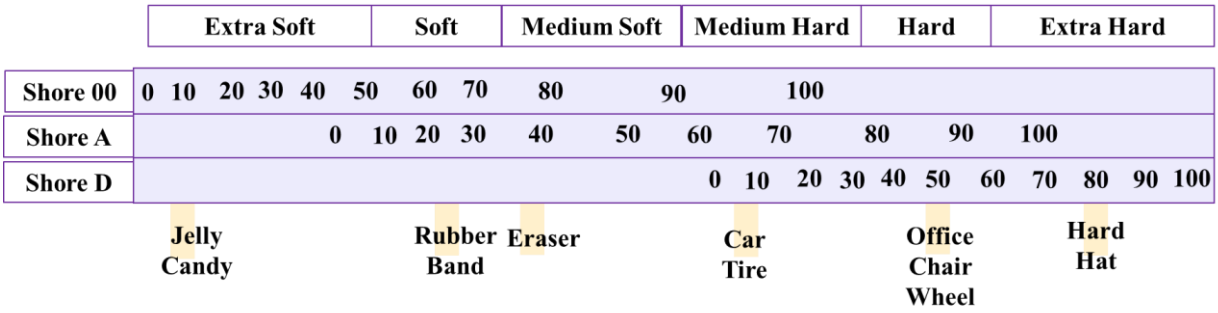

Figure 5: Durometer Shore Hardness scale of polymers [16]

1.1.4.2 Monitoring System

A monitoring system to control the amount of inflation of the dilator and the temperature of the warm saline water for inflating the dilator is needed for both doctors and patients to record the values that feel the most comfortable during therapy.

1.2 Engineering Background

In this thesis, we are focusing on the design and manufacturing of inflatable vaginal dilators. We measure the inflation of the dilator, determine the force that the dilator exerts on the vaginal wall when expanding, and determine the effect of wall thickness and design parameters of the dilator.

1.2.1 Design

In order to address the problem of selecting the correct dilator size, an inflatable dilator is desirable. In addition, painless insertion and use are important. Thus, a soft material to replace the hard plastic, latex or glass dilator is needed. A prototype of an improved dilator is shown in Figure 6. This dilator is made of soft silicone and can be expanded in size by increasing the internal pressure.

Figure 6: Current prototype of the vaginal dilator

1.2.2 Polymer Materials and Material Characterization Testing

1.2.2.1 Elasticity and Plasticity

When applying a force on a solid object, it will experience a deformation process. Within a small deformation range, an object can experience elastic deformation where the object can recover its original shape and size [17]. In the linear elastic deformation region, stress is

proportional to strain. If the stress exceeds a proportionality limit (point H in Figure 7), it can cause non-linear elastic or plastic deformations [52]. The main material properties to describe elasticity are elastic modulus and elastic limit [52]. Elastic modulus is a measure of the intensity of deformation, and the elastic limit indicates the critical point where permanent plastic deformations start, (point E, Figure 7(a)) [52]. If an object deforms beyond the elastic limit (Figure 7(a)), it will experience plastic deformation [18]. In the plastic deformation region, the material remains its deformed shape, [18]. For ductile materials, plastic deformation will always occur after elastic deformation, while for brittle materials, very little elastic deformation will occur before breakage [17].

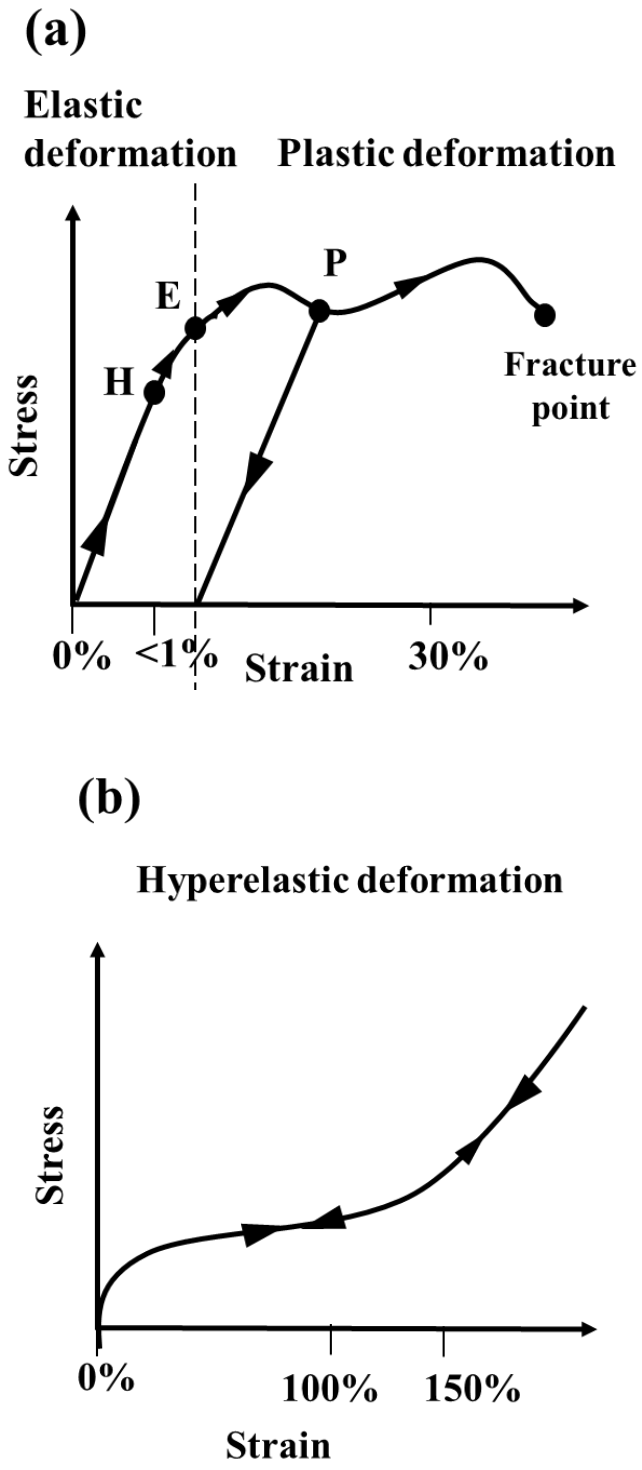

Figure 7: (a) Stress and strain response of a common material [52] and (b) stress and strain response of a hyperelastic material

Hyperelasticity is a special case of elasticity, where the material will respond elastically and nonlinearly under large deformation [53]. The characteristics of hyperelastic materials are: 1) the materials are deformable and recoverable, 2) the materials are nearly incompressible, and 3) the materials will show a highly nonlinear stress-strain relationship (Figure 7(b)) [53]. In general, the strain-energy function is used to describe the mechanical behavior of hyperelastic materials [19].

1.2.2.2 Constitutive Equations

Constitutive equations are used to describe the stress-strain response of any material. [21]. Special equations to characterize hyperelastic materials such as silicones have been derived [22]. The stress-strain relationships are determined by experimental studies. In this thesis, a two-term Mooney-Rivlin constitutive model was used for the characterization of silicone (Dragon Skin 10).

Several constitutive models have been used to fit hyperelastic materials, e.g., Mooney–Rivlin, Yeoh, Neo–Hookean, Ogden, Humphrey, Martins, and Veronda–Westmann [19]. Finding the best fit for the constitutive equation is a prerequisite for numerical simulations. Without accurate constitutive equations, finite element analysis is not reliable [20].

In order to characterize the mechanical properties of materials, uniaxial tensile testing experiments were performed. A commercially available uniaxial tensile testing machine (ESM303) was used to measure the stress-strain relationship of silicone. Digital Image Correlation (DIC) methods were used to determine the stress-strain relationship of the silicone material.

1.2.3 Finite Element Simulation

Finite element analysis (FEA) is the process of simulating the behavior of a part or assembly under given boundary conditions [23]. The finite element simulation method can be used to decrease the need for physical prototypes in the design process [24]. In addition, it can help to optimize the prototype during the design process [24]. In this thesis, finite element simulations were performed to provide a reasonable prediction of the inflation of the dilator.

1.2.4 Software

In this thesis, commercially available computer-aided design (CAD) software (SolidWorks) was used for the mechanical design of the prototype. Commercially available finite element analysis software (Altair Hypermesh) was used for meshing and assigning boundary conditions, and another commercially available finite element analysis software (LS-DYNA) was used to perform the time-dependent simulation.

1.2.5 Experimental Studies

In addition to the numerical simulations, experiments were conducted to measure the size of the dilator during inflation, and the force of the dilator that was exerted on the surroundings when inflated. From these two experiments, we were able to obtain a better understanding of the dimension of the dilator as a function of the pressure and estimate the force that the patient will experience during vaginal dilator therapy.

1.2.5.1 Setup of the Dilator and Vaginal Wall Force Recording and Inflation Experiment

To measure the relationship between dilator inflation and the force applied to the wall of the vagina, we used the experimental setup shown in Figure 38 and Figure 42, consisting of a load cell, actuator arm, pressure sensor, peristaltic pump, a set of 3D printed flat plates to simulate the vaginal wall, and a dilator. A digital camera was used to record the size and shape of the dilator during inflation. By measuring the cross-sectional area as a function of time. A microcontroller (Arduino Mega2560) was used to gather the data collected by the pressure sensor. A load cell was used to obtain the applied force of the dilator to the vaginal wall.

1.3 Thesis Objective

The objective of this thesis is to design and implement a soft and inflatable vaginal dilator. To achieve this goal, material selection and characterization are important considerations. Finite element simulation and experimental studies were used to determine the optimal thickness of the silicone balloon used in the dilator.

1.4 Organization of thesis

Chapter 1 introduces the medical background of cervical cancer, radiotherapy, and brachytherapy, and the problem patients encounter when performing vaginal dilator therapy. The engineering background of dilator design is introduced, along with material testing, numerical simulation, and experimental investigation.

Chapter 2 deals with the initial design of a single chamber dilator and introduces an improved dual chamber dilator design. The manufacturing process of the dilators will be discussed, and the design of the monitoring system to control the dilator's inflation will also be introduced.

Chapter 3 presents the results of the material testing of hyperelastic silicone materials for manufacturing vaginal dilators. Stress and strain data collected using a uniaxial tensile testing machine and Digital Image Correlation will be described. Mooney-Rivlin coefficients for a hyperelastic material will be obtained.

Chapter 4 discusses a numerical study of dilator inflation using the Mooney-Rivlin material coefficients of Chapter 3. Plots of pressure versus cross-section area and pressure versus load on a vaginal wall are obtained for silicone dilators with varying silicone wall thicknesses.

Chapter 5 shows the details of the experimental setup. Different wall thicknesses of silicone dilators will be displayed as a function of internal pressure. The experimental results are compared to the numerical studies performed in Chapter 4.

Chapter 6 will conclude the thesis with a summary and will provide future directions and goals for the project.

Chapter 2 Design and Fabrication of an Inflatable Balloon Dilator

2.1 Design Requirements

Commercially available dilators [25] are generally sold in a set of four to five with multiple graded diameters. Recently, an inflatable dilator was developed and commercialized. Inflation of the dilator is accomplished by a mechanism of spines and distal arms (Figure 8(b)) and can be controlled by means of a microcontroller [26]. The cross-section of the dilator changes into an asterisk-like shape upon inflation (Figure 8(a)) and does not fully stretch along the vaginal canal. Our design requirements are to improve the current commercial dilator into a fully expanding dilator capable of controlling independent sections of the dilator.

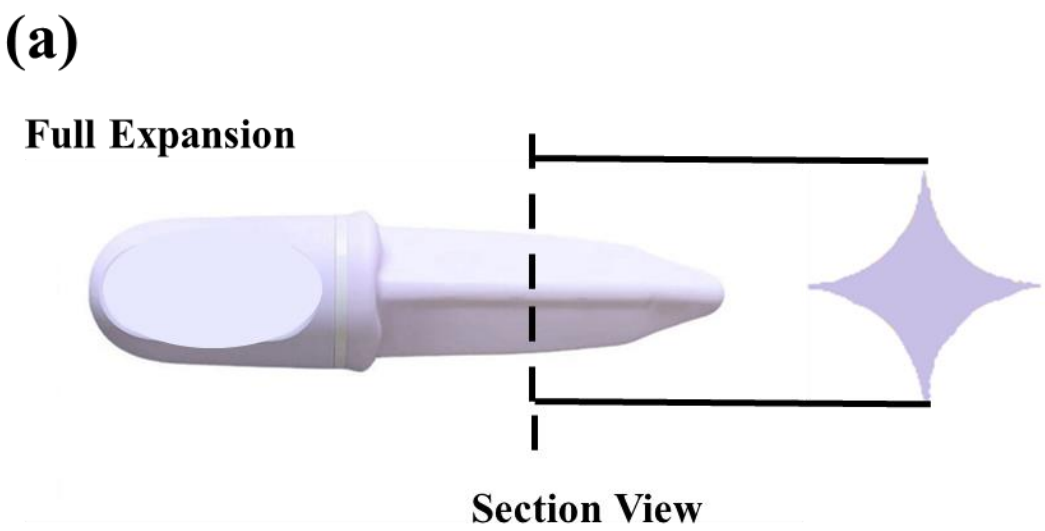

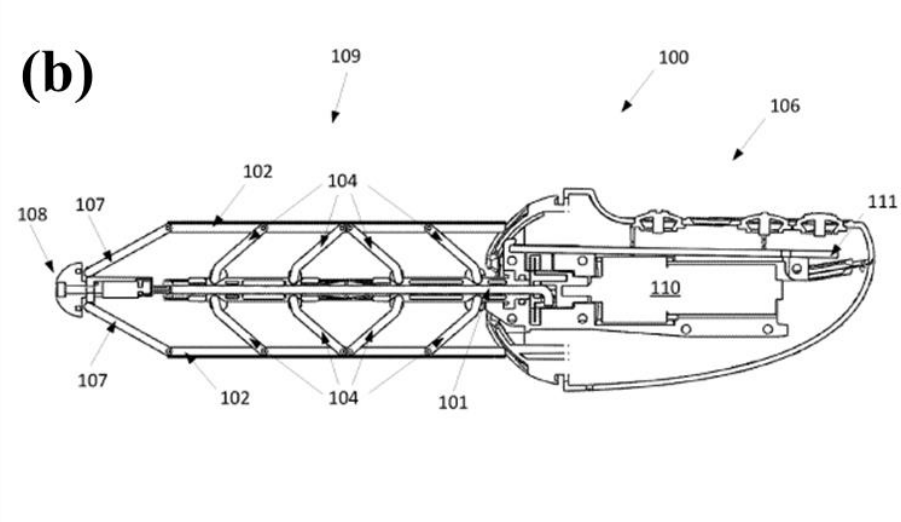

Figure 8: (a) Cross-sectional view of the inflatable vaginal dilation device (b) Mechanism of the inflatable vaginal dilation device [5]

2.2 Initial Design of an Inflatable Balloon Dilator

The initial design of our new dilator was inspired by an existing vaginal stent prototype [27]. This vaginal stent was made of polyurethane foam with a dimension of 255 mm in length, 145 mm in width, and 3 mm in thickness. The polyurethane foam was covered with a latex condom with the inflation tubing exiting the open end of the condom [27]. Our initial prototype was a 3D printed model with the shape of a commercial dilator and covered with a thin layer of silicone. This initial device did not inflate well due to sealing problems and uneven silicone layer thickness. Figure 9 shows the initial design of the vaginal dilator.

Figure 9: Initial design of the vaginal stent

2.3 Single Chamber Inflatable Balloon Dilator

The initial design of the dilator was improved by the use of a 3-part mold (Figure 10), which allowed the control of the wall thickness of the dilator. After the mold was manufactured, a rod was used to maintain the shape of the dilator. In order to inflate the dilator, air channels (Figure 11) were incorporated.

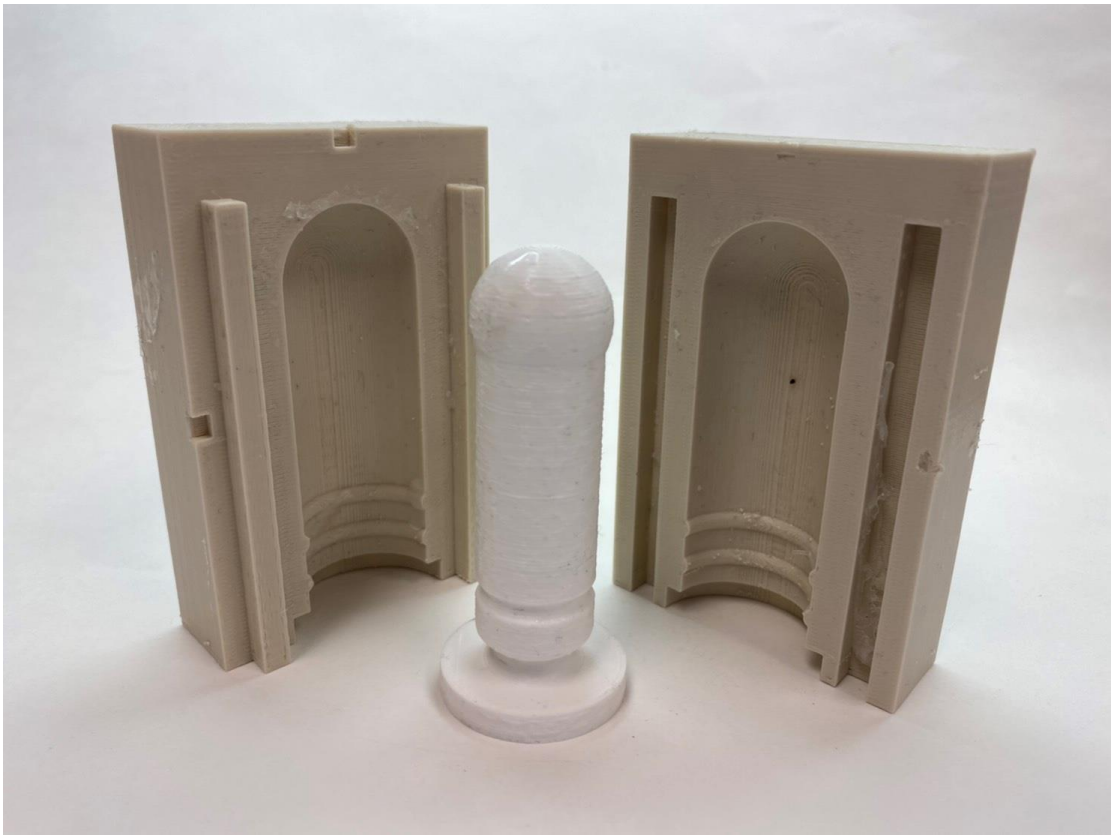

Figure 10: First iteration of 3-part mold design

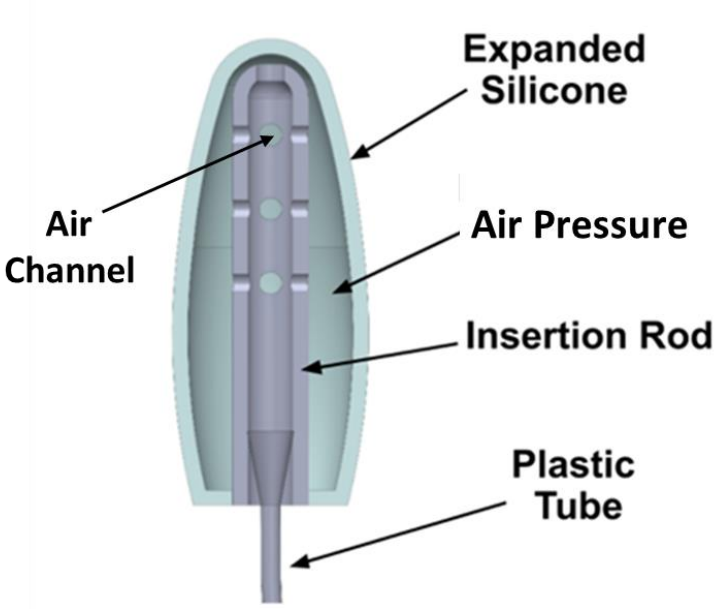

Figure 11: Cross-section model of dilator design [47]

2.3.1 Manufacturing Process of Single Chamber Dilator

The first step in manufacturing the vaginal dilator was to design a three-part mold. The dimensions of the three-part mold are shown in Figures 12 and 13. The manufacturing of the mold was performed using 3D printing. Parts designed in computer-aided design software (Solidworks) were exported to the Slicer software for 3D printing. A commercially available 3D printer was used to fabricate the three-part mold. After printing and postprocessing the mold, silicone was poured into the mold and the inner rod was inserted. An inner rod with holes was designed and 3D printed to serve as an air channel. After the silicone was cured, the thin silicone membrane obtained from the mold, the inner rod with air channels, and the inflation tube were assembled. A zip tie or rubber band was used at the groove position to prevent leakage when inflating the dilator. Figure

14 shows the steps needed for manufacturing a vaginal dilator and Figure 15 shows the assembled dilator.

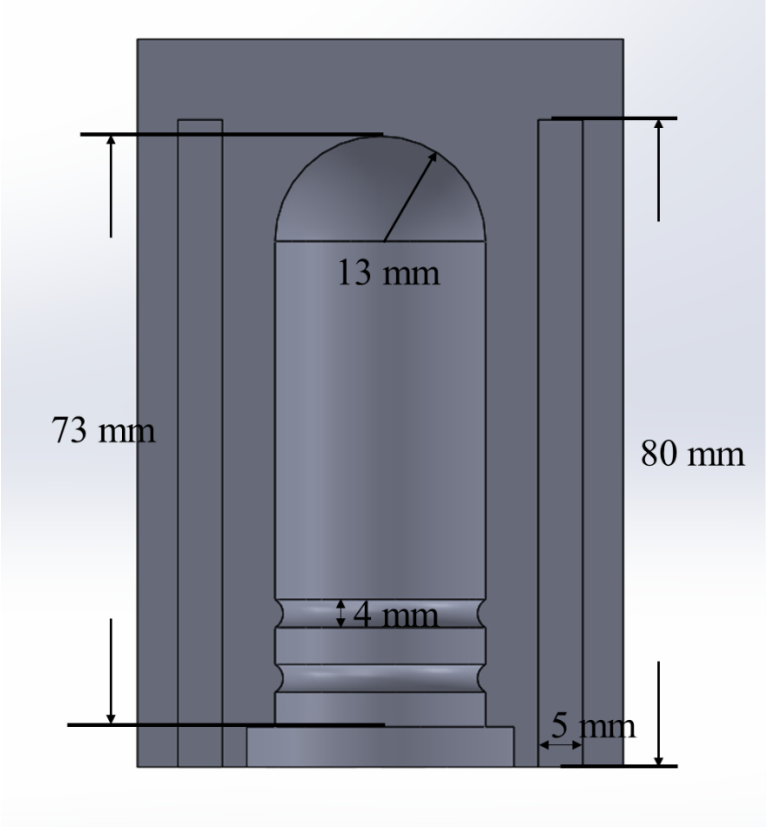

Figure 12: Single chamber dilator mold (outer case) with dimensions

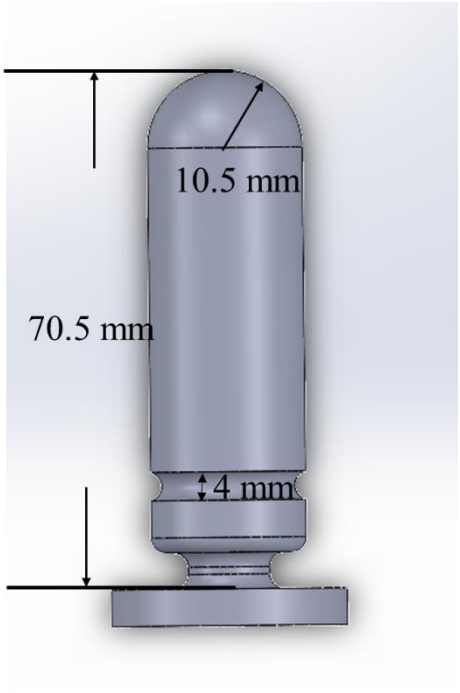

Figure 13: Dilator mold (inner rod) with dimensions

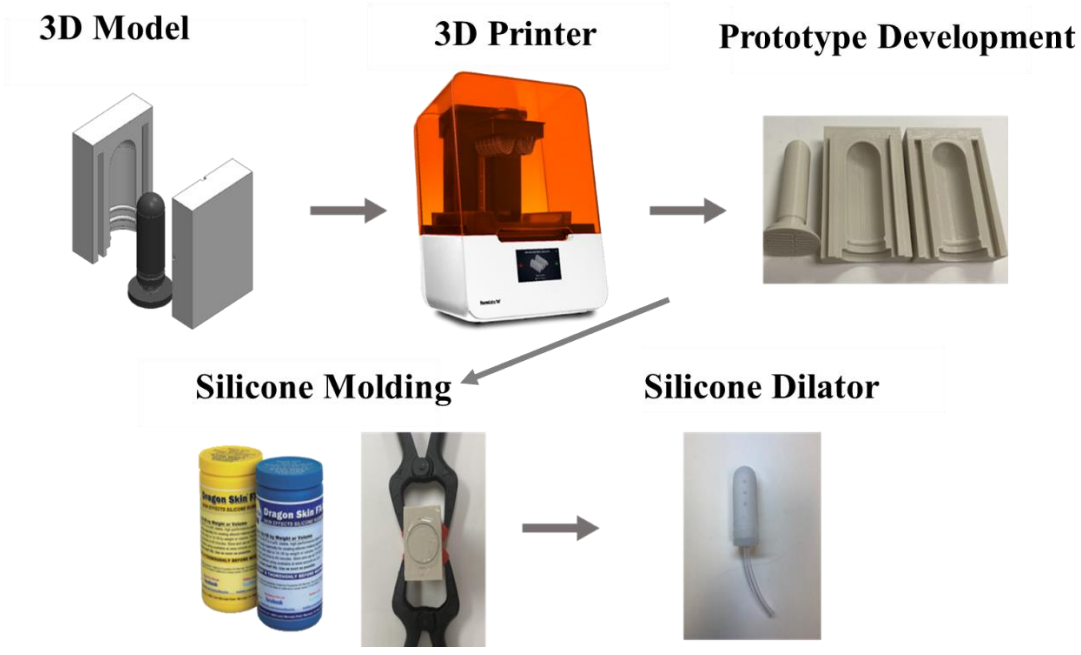

Figure 14: Manufacturing steps of the vaginal dilator

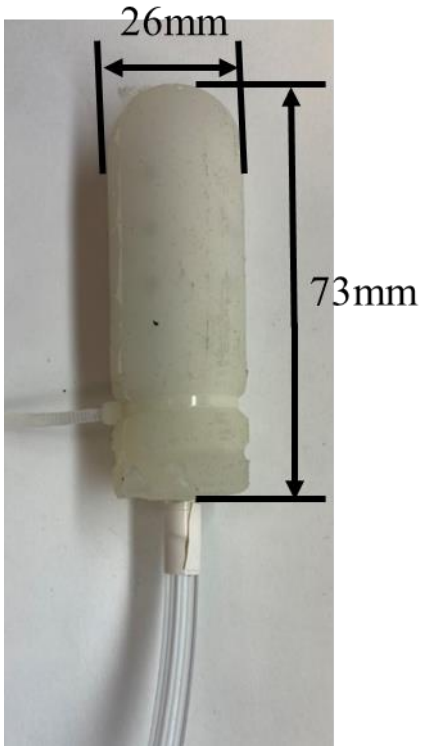

Figure 15: Single chamber vaginal dilator

The single chamber dilator was improved by sealing the base of the dilator with extra silicone. In addition, the dimensions of the dilator were reduced (Figure 16). The scaled-down design was similar in dimensions to commercially available hard plastic dilators of smaller diameters. A 3mm diameter cylinder was added at the apex of the mold for centering the inner rod in the three-part mold and improving the accuracy of the silicone wall thickness. Figure 17 shows the design of the dilator that was used for all subsequent experiments and tests.

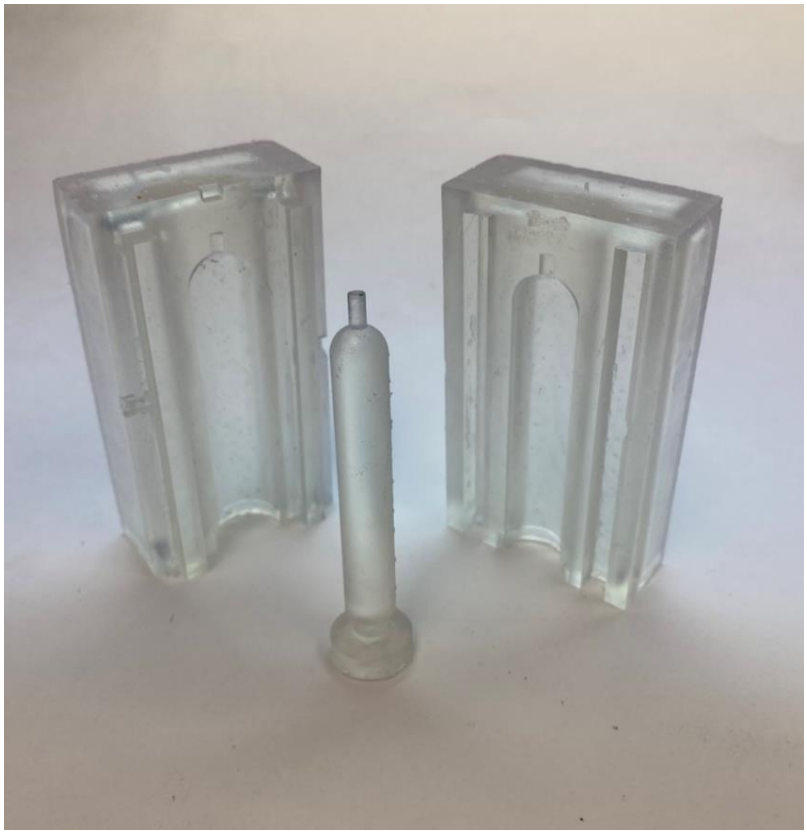

Figure 16: Mold of vaginal dilator

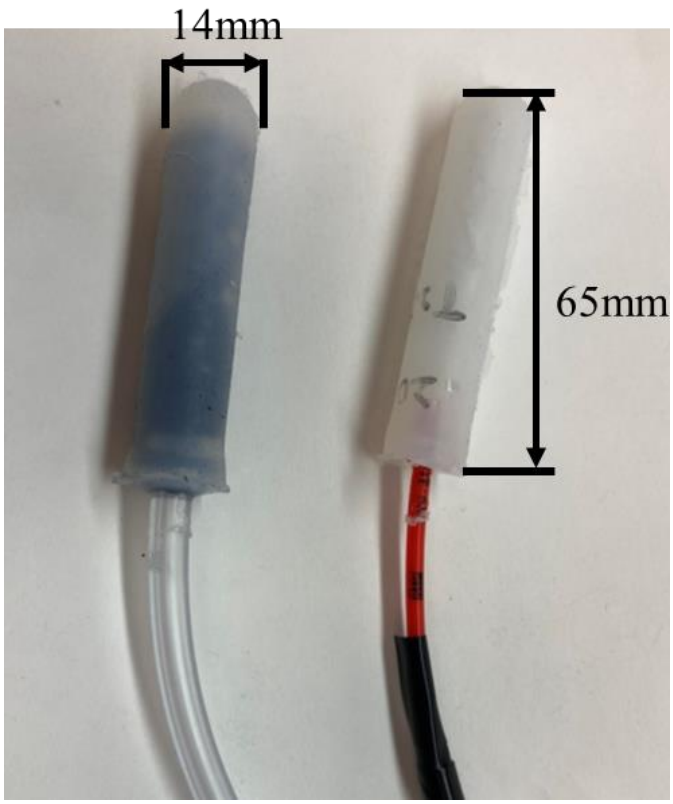

Figure 17: Assembled vaginal dilator

2.4 Dual Chamber Inflatable Balloon Dilator

A schematic of a dual chamber vaginal dilator design is shown in Figure 18(a). Compared to the single chamber dilator, a dual chamber dilator permits inflation and control of two individual sections of the dilator (Figure 18(b)). The advantage of this design is that it allows the dilator to address locations in the vagina where stenosis is most serious. The manufacturing steps for fabricating a dual chamber dilator are similar to those of a single chamber dilator. However, two different molds are needed to fabricate the apex part of the dilator separately from the base part of the dilator. The manufacturing steps are as follows: 1) design and print the mold for the apex part of the dilator shown in Figure 19 and Figure 20; 2) pour silicone into the 3-part

mold; 3) cure silicone; 4) and insert the inner rods with the tube into the silicone sheet and seal the base of the dilator with silicone. The base part of the dilator is created by repeating steps 1 through 4 using silicone. The dimensions of the 3-part mold for manufacturing the base chamber of the dilator are shown in Figures 21(a)-(b).

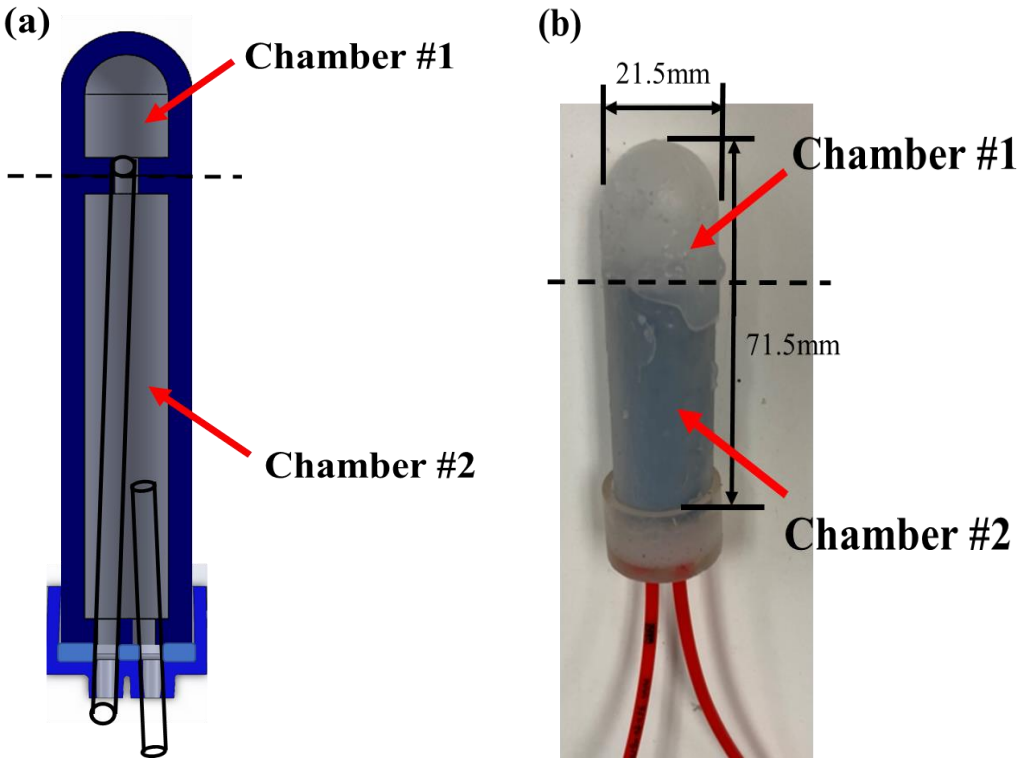

Figure 18: (a) Schematic of a dual chamber dilator and (b) an improved design of dual chamber dilator

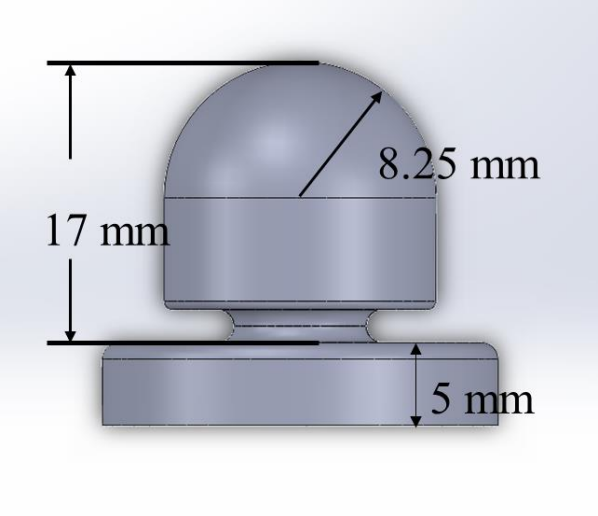

Figure 19: 3-part mold inner rods with dimensions labeled

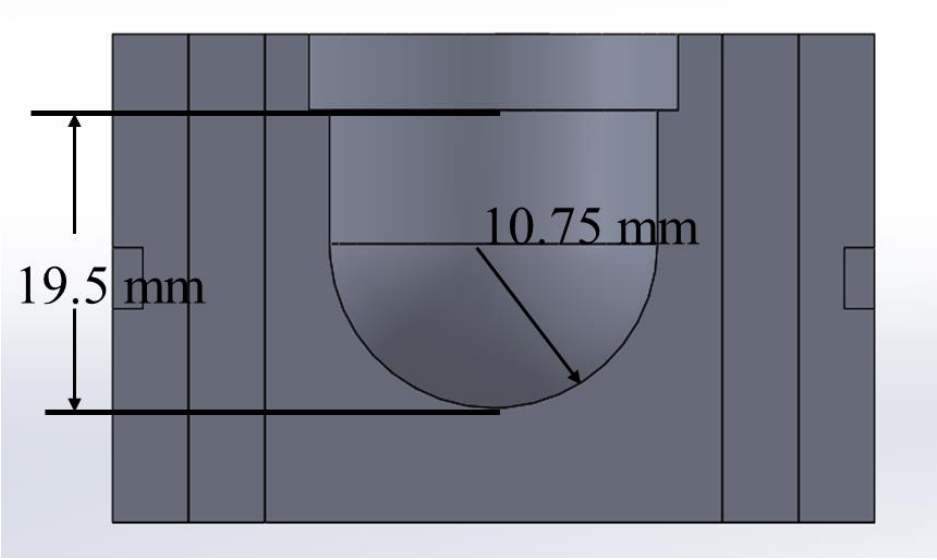

Figure 20: 3-part mold apex part with dimensions labeled

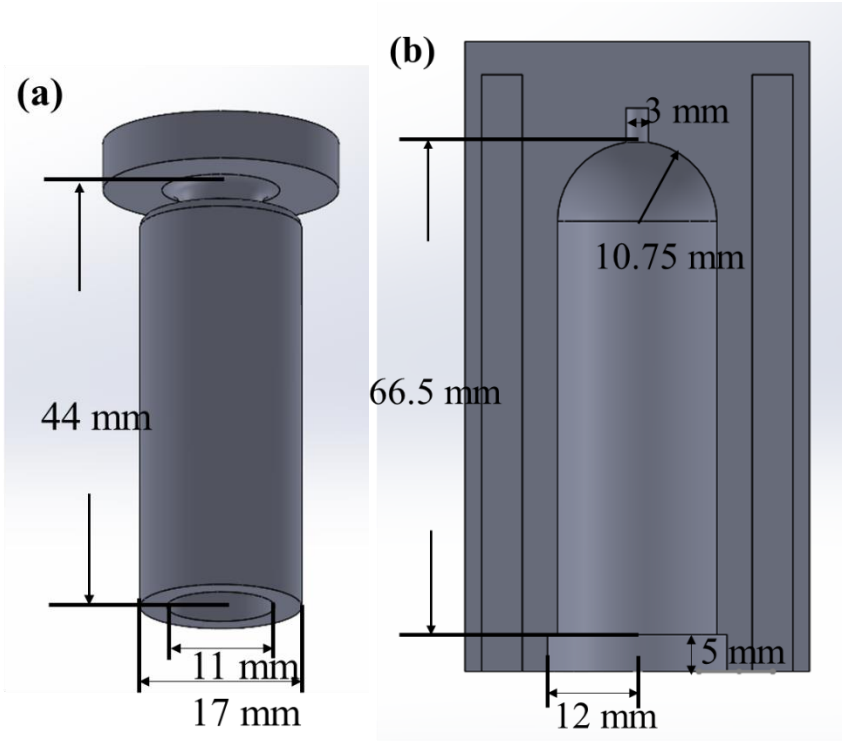

Figure 21: (a) 3-part mold double chamber inner rods and (b) 3-part mold double chamber base case

2.5 Reliability of Inflatable Balloon Dilator

One of the main problems with vaginal dilators is the leaking of air when inflated. Leaking is related to incomplete sealing due to variations in the thickness of the dilator wall, and bubble formation in the silicone during the manufacturing process. Modifying the design of the tip of the inner rod improved the uniformity of the dilator wall thickness.

Another cause of leakage was found to be insufficient sealing between the tube and the silicone dilator (Figure 11). This problem was initially solved with the use of a zip tie or rubber band to tighten the silicone dome. For later designs, we used a dilator cap injected with silicone to

seal the gap between the dilator cap and the dilator. This created a thick silicone layer that prevented leaking.

2.5.1 Vaginal Dilator Accessories

Both the single chamber and the dual-chamber dilator caps shown in Figures 22(a) and 22(b) cover the base of the dilator. A hole of a diameter of 3.5 mm was used into inject silicone to the cap of the dilator to reduce leaking (Figure 23).

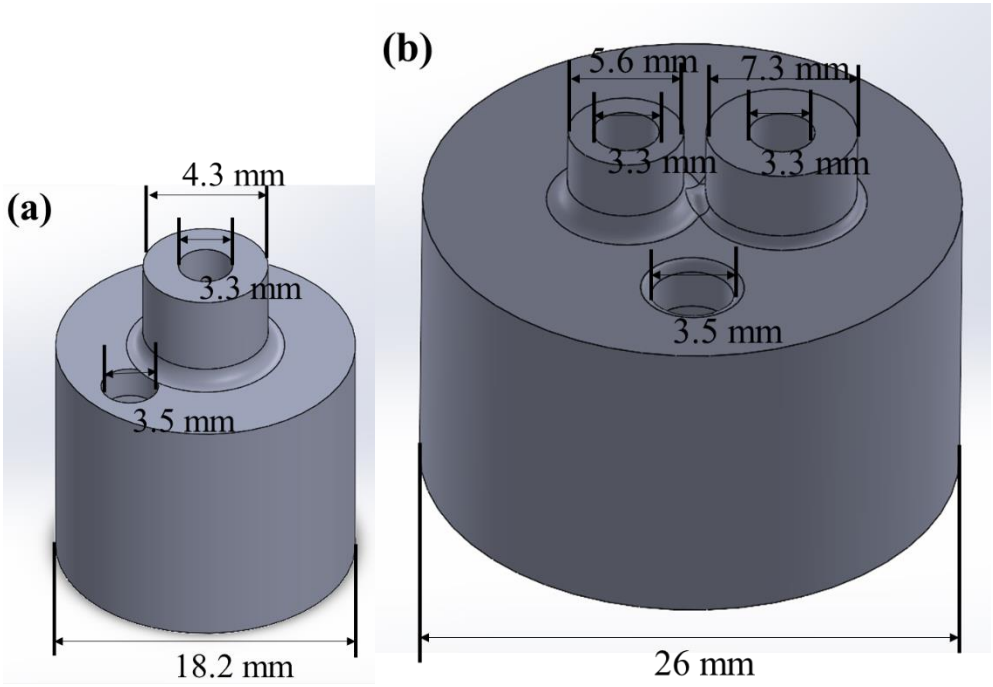

Figure 22: (a) One chamber dilator cap and (b) Two chamber dilator cap

Figure 23: Silicone injection into the dilator cap

The dilator handle was designed so that a patient can hold the dilator easily during dilator therapy. Figure 24 shows the assembled dilator handle and dilator.

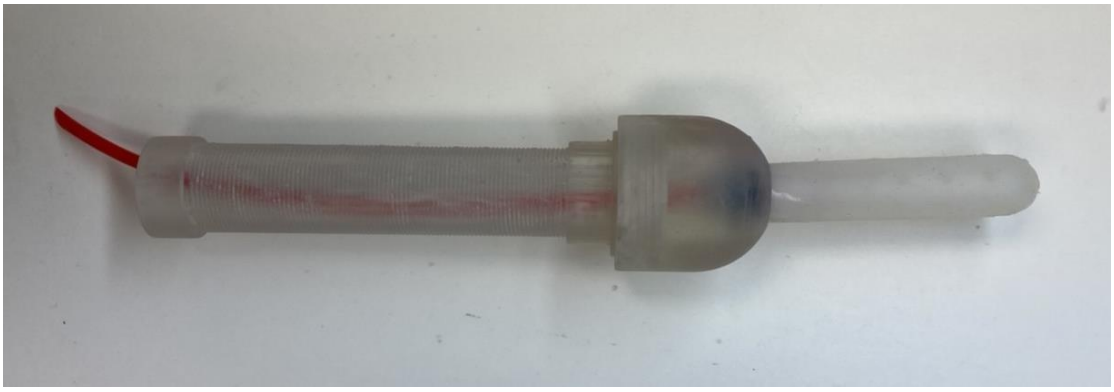

Figure 24: Dilator handle with dilator

2.6 Design and Manufacturing of the Dilator Monitoring System

A monitoring system was developed to measure the pressure, flow rate, and temperature of the dilator during inflation. Two different frequencies were used comparing to different severity of vaginal stenosis. The aim of designing a monitoring system is to give doctors and patients information about the effectiveness of dilator therapy with a minimum level of pain, which will help determine the design and performance specifications of the dilator.

2.6.1 Overview of Monitoring System

The housing of the monitoring system was designed to incorporate the microcontrollers, sensors, and monitors to display the sensor data. A flow sensor, a temperature sensor and a pressure sensor were used to collect data for the flow rate, the temperature of the fluid, and the pressure of the inflating dilator, respectively. Three microcontrollers (Arduino mega 2560) were used to gather data from three sensors and to display the measurements recorded in real-time [62]. Control buttons were used for modifying the frequency of inflation and deflation, respectively, and the overall therapy time [62]. Two sets of pumps and valves were used to move the liquid and maintain a steady pressure when the pump stops inflating the dilator [62]. A micro-SD card slot was used to help save and output the data collected from the sensor. A cylindrical reservoir was attached to the monitoring system case and connected with plastic tubes to provide enough liquid to inflate the dilator. Two power adapters were used for providing power to the microcontroller and to the pumps and valves. The housing was split into upper and lower sections. Electronic components

were seated on the upper section, while the pump and the valve were located in the lower section of the case. Figure 25 shows the overall design of the housing and Figure 26 shows the actual monitoring system manufactured.

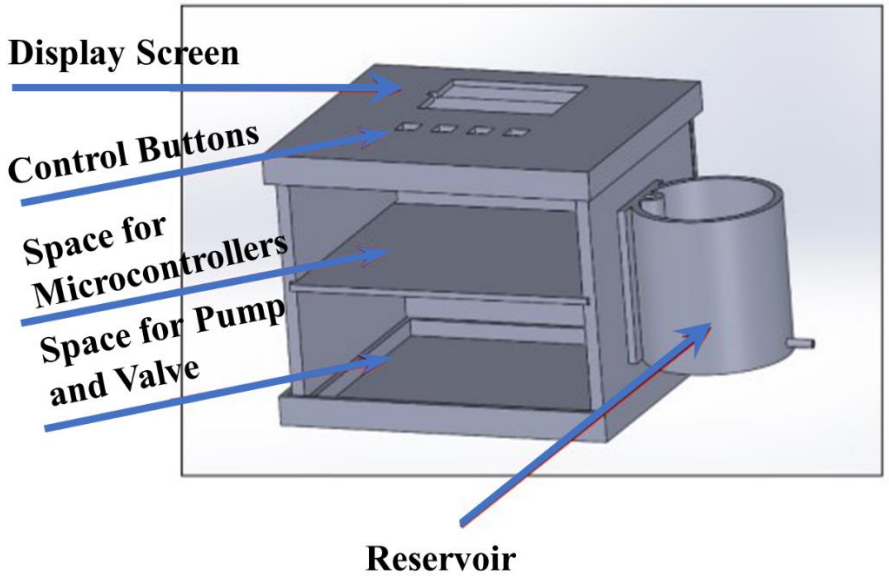

Figure 25: CAD model of the case of the monitor system and brief description

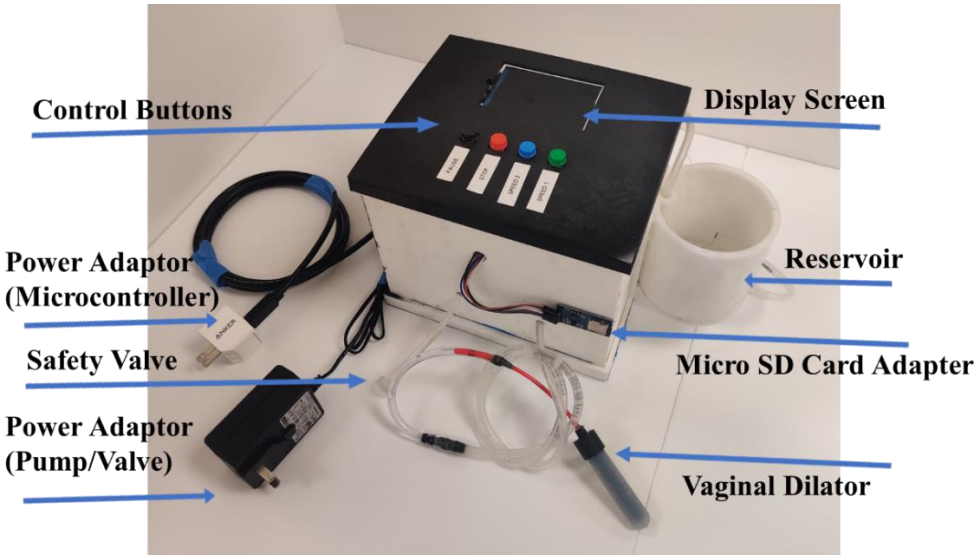

Figure 26: Actual monitor system and the combination of vaginal dilator [62]

The steps of using the dilator and the monitoring system to perform vaginal dilation therapy are as follows. 1) Connect the dilator to the monitor system. 2) Connect the power adapters to a power supply, and check that the monitor lights up. Make sure there is a micro-SD card in the card reader slot to store the data. 3) Pour warm saline solution into the reservoir. 4) Insert the vaginal dilator to the vagina with lubricant. 5) Choose a suitable therapy mode and start the therapy. For patients that have more advanced vaginal stenosis, a therapy mode where the dilator does not expand too much or too fast will be more suitable, with the opposite applying to less severe cases of vaginal stenosis.

Chapter 2 and Chapter 4, in part, contains published material as it appears in Rafaela Simoes-Torigoe, Po-Han Chen, Yu M. Li, Matthew Kohanfars, Karcher Morris, Casey W. Williamson, Milan Makale, Jyoti Mayadev, Frank Talke, "Design and Validation of an Automated Dilator Prototype for the Treatment of Radiation Induced Vaginal Injury," 2021 43rd Annual International Conference of the IEEE Engineering in Medicine & Biology Society (EMBC), IEEE. The thesis author was a co-author of this paper.

Chapter 2, in part, contains unpublished material as it appears in Shengfan Hu, Karcher Morris, Po-Han Chen, Rafaela Simoes-Torigoe, Yu M. Li, Milan Makale, Jyoti Mayadev, Frank Talke, "A Soft Robotic Closed-Loop System for the Treatment of Vaginal Stenosis," 2022 JSME-IIP/ASME-ISPS Joint International Conference on Micromechatronics for Information and Precision Equipment (MIPE2022). The thesis author was a co-author of this paper.

Chapter 3 Uniaxial Tensile Testing of Hyperelastic Polymers

3.1 Properties of Elastomers

The silicone that is being used for fabricating the dilator is an elastomer. An elastomer is a polymer that experiences large reversible strain in response to applied stress [28]. In this thesis, the silicone elastomer used will be tested to determine its mechanical characteristics. Figure 27 shows the difference in the stress-strain curve between a linear elastic material and a hyperelastic material. Linear elastic materials have stress values proportional to strain. Hyperelastic materials respond elastically but respond nonlinearly under deformation.

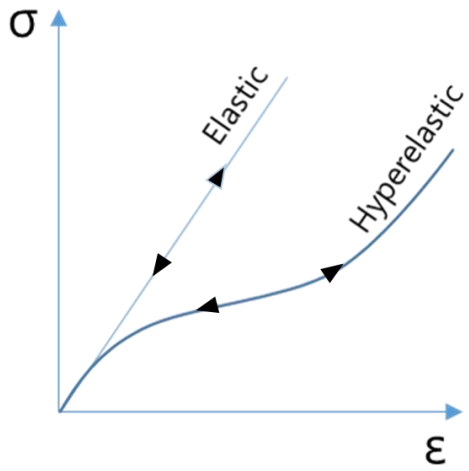

Figure 27: Stress-strain curve of elastic and hyperelastic material [51]

Silicone elastomers have good thermal stability, low electrical conductivity, and are generally biocompatible. [29]. Silicone polymers have a backbone of alternating units of silicon

and oxygen, which causes high flexibility and high thermal stability [30]. A general chemical formula for typical silicone elastomers is shown in Figure 28, the symbol ‘R’ in Figure 28 denoting the organic group that is attached to the silicone backbone. Silicone polymers and other amorphous polymers increase in their elastic response when cross-linked [31]. Compared to plastics, elastomers have a great capacity for large elastic deformation under applied stress, and they can be stretched over 100% of their original length with no permanent deformation [32]. Common silicone elastomers can be classified into three categories based on their curing temperature: room temperature vulcanizing (RTV), high temperature vulcanizing (HTV), and liquid silicone rubber (LSR) [31]. Most commercial silicone elastomers are mixed with a crosslinker and a base or a polymer, and are typically crosslinked using hydrosilylation, condensation, or radical reaction [31].

Hydrosilylation is the insertion reaction of an unsaturated vinyl group into a silicon hydrogen bond [54]. Condensation of a polymer means that its monomers or oligomers react with each other to form larger units and will release smaller molecules (water) during the reaction [55]. The free radical reaction is an addition of free radicals that takes place to form the polymer unit. [56]

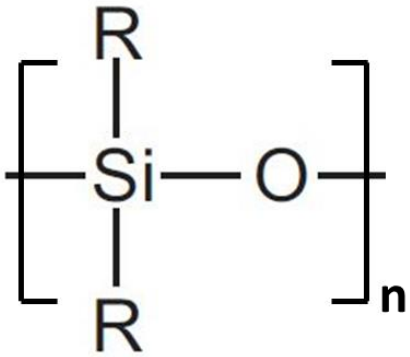

Figure 28: General chemical formula of silicone [57]

3.2 Introduction to Hyperelastic Models

The nonlinear stress-strain relationship exhibited by hyperelastic materials such as silicone elastomers requires specialized constitutive models to describe their mechanical behavior [22]. Hyperelastic models depend on experimentally determined variables. A number of models for the constitutive equations of hyperelastic materials have been proposed using various material parameters [32]. Among the most popular constitutive models are the so-called Neo-Hookean model, the Mooney-Rivlin model, the Ogden model, the Yeoh model, the Fung-Demiray model, and the Veronda-Westmann model, the Arruda-Boyce model, and the Gent model [34]. For the derivation of the constitutive equations of the various models, the materials were assumed to be isotropic and incompressible. Least square methods are generally used to calculate the best fit for a material coefficient from experimental measurements. The constitutive equation can later be used for finite element analysis.

The Mooney-Rivlin model is one of the most widely used models for hyperelastic materials [35]. This model characterizes the mechanical behavior of rubber materials at small and medium elongations [35]. Several forms of the Mooney-Rivlin model exist in the literature, and they are categorized by their number of material parameters in the equation [36]. In deriving the Mooney-Rivlin model, the strain energy density function W is used.

$$W(I_1, I_2) = C_1 (I_1 - 3) + C_2 (I_2 - 3) \tag{3.2.1}$$

In Equation 3.2.1, the coefficients C_1 and C_2 are the so-called Mooney-Rivlin material coefficients, while I_1 and I_2 are the principal invariants defined by using the left Cauchy–Green deformation tensor, D_R, and the principal extension ratios λ_1, λ_2, and λ_3 [37]. The left Cauchy–Green deformation tensor is defined as $D_R = FF^T$, where F is the deformation gradient and ^{T} denotes the

transpose [58][59]. If one assumes that the principal extension ratio $\lambda_1 = \lambda$, and the material is incompressible $\lambda_1\lambda_2\lambda_3 = 1$, we obtain $\lambda_2 = \lambda_3 = \frac{1}{\sqrt{\lambda}}$. Here, λ is the normalized elongation of the coupon specimen and ε is the strain of the coupon specimen, $\lambda = 1 + \varepsilon$ [36] [37]. F is defined as,

$$\mathrm{F} = \begin{bmatrix} \lambda_1 & 0 & 0 \\ 0 & \lambda_2 & 0 \\ 0 & 0 & \lambda_3 \end{bmatrix} = \begin{bmatrix} \lambda & 0 & 0 \\ 0 & 1/\sqrt{\lambda} & 0 \\ 0 & 0 & 1/\sqrt{\lambda} \end{bmatrix} \tag{3.2.2}$$

and D_R as,

$$D_R = \begin{bmatrix} \lambda_1^2 & 0 & 0 \\ 0 & \lambda_2^2 & 0 \\ 0 & 0 & \lambda_3^2 \end{bmatrix} = \begin{bmatrix} \lambda^2 & 0 & 0 \\ 0 & 1/\lambda & 0 \\ 0 & 0 & 1/\lambda \end{bmatrix} \tag{3.2.3}$$

The I_1 and I_2 strain invariants are:

$$\mathrm{I}_1 = tr(D_R) = \lambda_1^2 + \lambda_2^2 + \lambda_3^2 \tag{3.2.4}$$

$$\mathrm{I}_2 = \frac{1}{2}[tr(D_R^2) - (tr(D_R^2))^2] = \lambda_1^2\,\lambda_2^2 + \lambda_2^2\,\lambda_3^2 + \lambda_3^2\,\lambda_1^2 \tag{3.2.5}$$

where "*tr*" is the trace operator of the matrix, and "*det*" the determinant operator of the matrix [60]. Inserting equation 3.2.4 and 3.2.5 into equation 3.2.1, we obtain

$$\mathrm{W}(\mathrm{I}_1, \mathrm{I}_2) = \mathrm{C}_1(\lambda^2 + \frac{2}{\lambda} - 3) + \mathrm{C}_2(2 + \frac{1}{\lambda} - 3) \tag{3.2.6}$$

The stress (σ) and elongation of the Mooney–Rivlin model is obtained by performing the differentiation of equation 3.2.6 with respect to the elongation [61].

$$\sigma = \lambda \frac{\partial W}{\partial \lambda} = 2\, C_1 \left(\lambda^2 - \frac{1}{\lambda}\right) + 2\, C_2 \left(\lambda - \frac{1}{\lambda^2}\right) \quad (3.2.7)$$

In equation 3.2.7, the coefficients C_1 and C_2 are the so-called Mooney-Rivlin coefficients.

3.3 Inadequate and Inconsistent Mooney-Rivlin Material Parameter of Silicone

The existing literature provides very few details about the two-term Mooney-Rivlin model for silicone that we are using in this thesis. Two papers were found with the value for the two-term Mooney-Rivlin model for silicone [38] [39]. Gopesh [38] performed a biaxial test with thin films of hyperelastic material. He determines the Mooney-Rivlin coefficients for commercially available silicone (Dragon Skin 10) to be C_1=0.18 MPa and C_2=0.0117 MPa [38]. In Lecce's paper, coefficients of C_1=0.12 MPa and C_2=-0.097 MPa were used for the same material (Dragon Skin 10) [39]. From these two papers, the difference in the parameters is large, indicating that the stiffness of the same material is quite different. Clearly, without accurate parameters for the silicone used, it would be impossible to perform an accurate finite element analysis calculation. Thus, we decided to perform experimental measurements of the stress-strain relationship to determine the Mooney-Rivlin coefficients for our silicone dilator.

3.4 Uniaxial Tensile Testing of the Silicone

Experiments were set up to obtain stress and elongation measurements for commercially available silicone (Dragon Skin 10) used for our vaginal dilator prototype. A commercially

available uniaxial tensile tester (in accordance with ASTM D412 standards) and a camera were used, as shown in figure 29(a)-(b). Dog-bone specimen (Figure 29(c)) for the tensile strength test was fabricated in accordance with ASTM D412 standards [40]. Digital image correlation, a non-contact optical technique to measure the deformation of the material, was implemented to measure elongation. Stress was calculated by dividing the load from the uniaxial tensile experiment by the cross-sectional area of the dog-bone specimen.

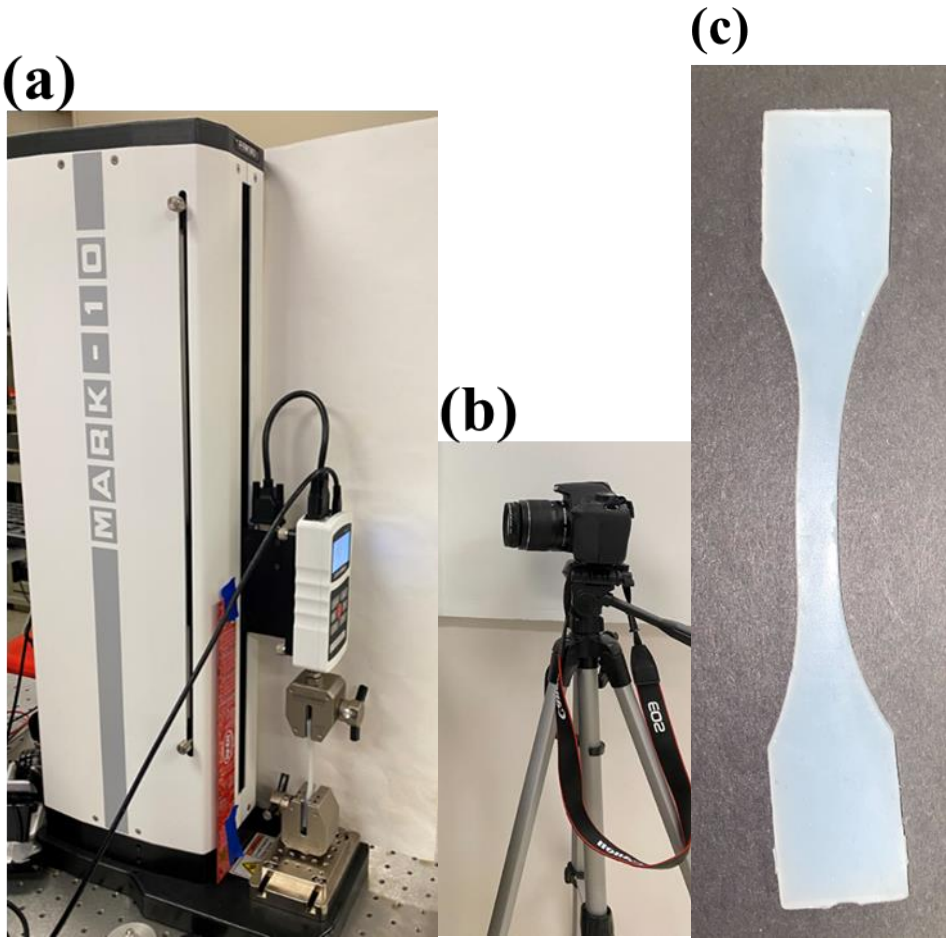

Figure 29: (a) Uniaxial tensile tester, (b) a camera, and (c) a dog bone specimen

3.4.1 Stress and Elongation Result of Silicone

In Figure 30, we show the stress versus elongation measurements for the silicone used in our work. Our observation of the data confirms that the silicone matches the hyperelastic behavior seen in Figure 27. Least square analysis was used for obtaining the two-parameter Mooney-Rivlin coefficient. The green curve in Figure 31 shows the two-parameter Mooney-Rivlin fit, indicating good agreement with experimental data. The Mooney-Rivlin coefficients of the silicone obtained from our tests are C_1= 0.026 MPa and C_2= 0.0093 MPa.

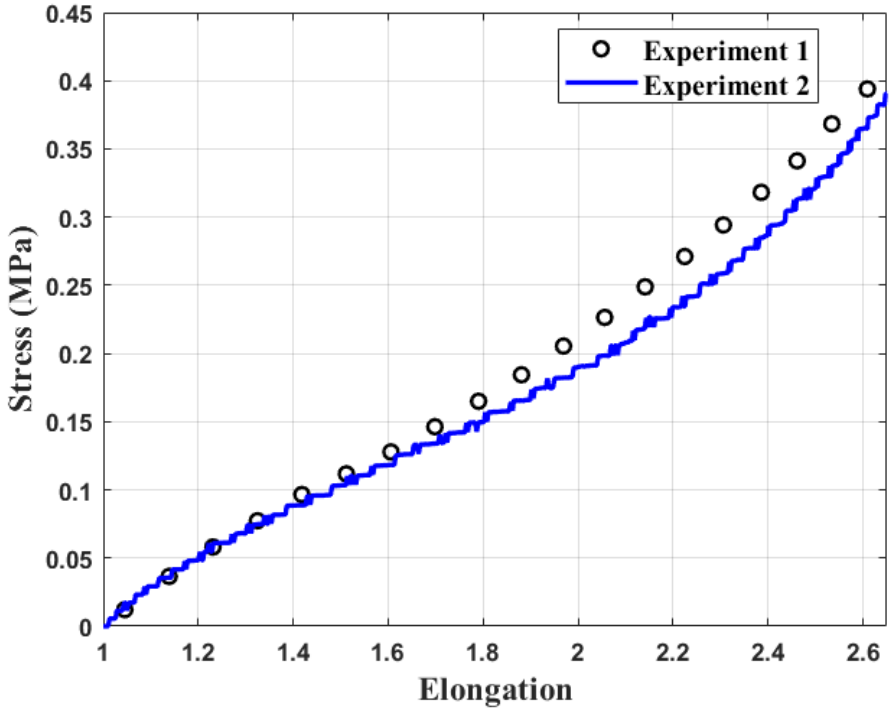

Figure 30: Experimental data of stress versus elongation of silicone

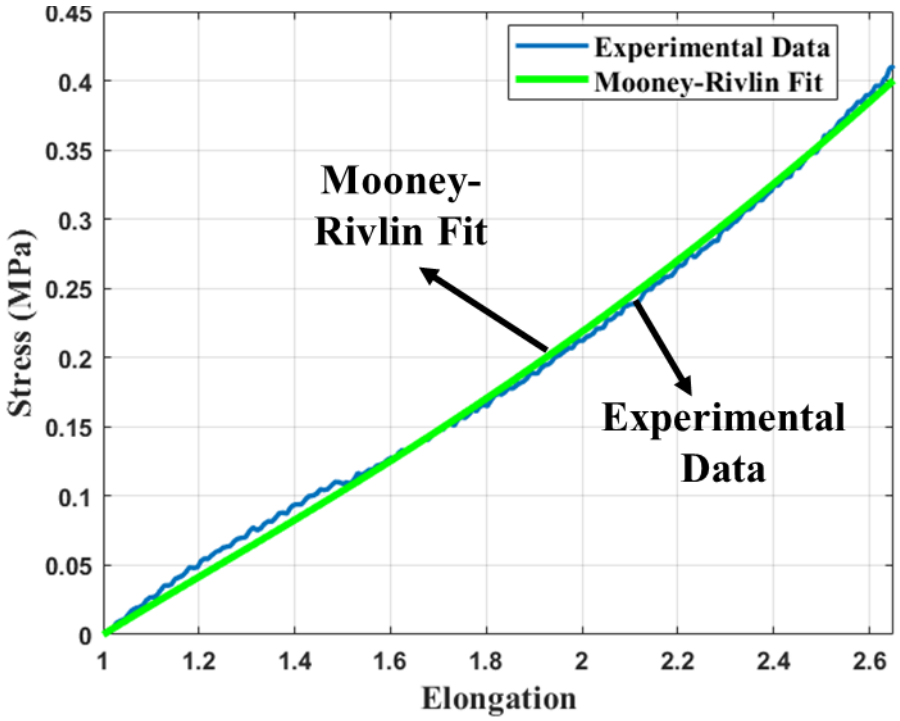

Figure 31: Stress-elongation experimental data and Mooney-Rivlin fit for silicone

The reason that the Mooney-Rivlin parameter of Gopesh et al [38] 2 term was different from our measurements might be due to the different fabrication techniques used for the same material. (Figure 32) This includes manufacturing temperature, cure duration, the sample's thickness, and the strain interval. In order to run an accurate finite element simulation, the testing of the material parameters should ideally be performed for the same manufacturing condition as those of the prototype.

Figure 32 shows the stress versus elongation plot for the experimental measurement along with the data reported by Leece et al. and Gopesh et al [38][39]. We observed that our Mooney-Rivlin parameters fit well with Leece's data for the strain interval from 0 to 1 [39] [41].

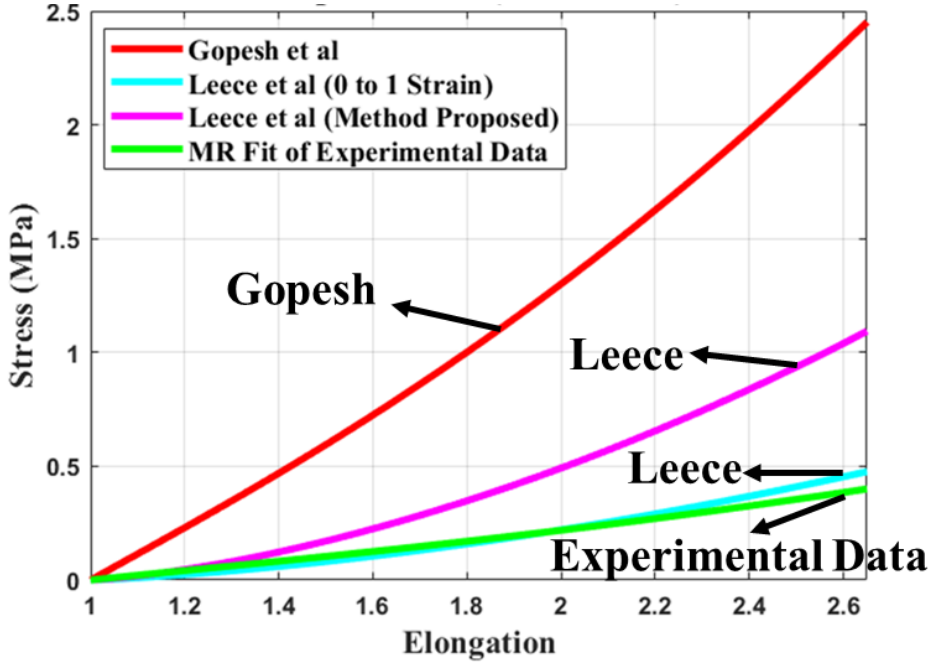

Figure 32: Stress-elongation plot of two term Mooney-Rivlin curve fit [38] [39]

Chapter 4 Numerical Study of Inflatable Balloon Dilator

4.1 Introduction of Finite Element Analysis

Finite Element Analysis is a numerical method for simulating physical phenomena with complex boundary conditions and material properties [23] [43]. It can be applied to various kinds of engineering problems, including structural or fluid flow, thermal transport, and mechanical systems [44]. The principle of finite element analysis is to discretize a model of the system into finite elements to estimate the value of the independent variable at the nodes of elements [23].

The advantage of using finite element methods is that engineers can reduce the number of physical prototypes and can optimize their designs by performing simulation studies [45]. The designs can easily be adjusted by changing dimensions, constraints, material properties, and repeating the calculations. Using the finite element method, one can reduce the manufacturing time and cost of developing a product.

The four main steps of finite element analysis are: 1) discretizing the solution region into a finite number of elements, 2) deriving governing equations for a typical element, 3) assembling all elements in the solution region, 4) and solving the system of equations obtained [46]. In this thesis, finite element analysis was used to simulate the inflation of the dilator to predict the displacement of the dilator and the force exerted on the vaginal wall. Finite element analysis software (Altair Hypermesh) was used to perform the preprocessing for finite element analysis,

including meshing, assembling of all elements, and applying material properties. Another commercially available finite element analysis software (LS-Dyna) was used to run the simulations to determine the deformation of the dilator as the function of time.

4.2 Effect of Wall Thickness of Vaginal Dilator

The characteristics of an ideal inflatable vaginal dilator are:1) a small initial pre-inflated size so that it can be inserted easily into the vagina, 2) slow and gentle dilator inflation for not causing pain during therapy, 3) the dilator should be able to inflate to reach the size of commercially available vaginal dilators, and 4) the pressure inside the dilator should be low to increase reliability during free inflation. Four different wall thicknesses of silicone dilators were evaluated to address the above points. (2mm, 2.5mm, 3mm, and 3.5mm respectively)

4.2.1 Finite Element Model

Figure 33 shows the geometry of the vaginal dilator and the vaginal wall with boundary conditions and applied pressure. In the simulations, four values of silicone wall thickness were considered (2mm, 2.5mm, 3mm, and 3.5mm). A six-degree of freedom constraint was implemented at the base of the dilator to prevent the dilator from moving, and a three-degree of freedom (rotation of X, Y, and Z axis) constraint was used at the tip of the dilator to prevent the dilator from rotating. The vaginal canal in the simulation was a simplified model and the vaginal width was controlled to be 15mm. The dilator has meshed with approximately 30,000 tetrahedral elements. At the beginning of the simulation, we assume that the dilator does not contact the vaginal wall.

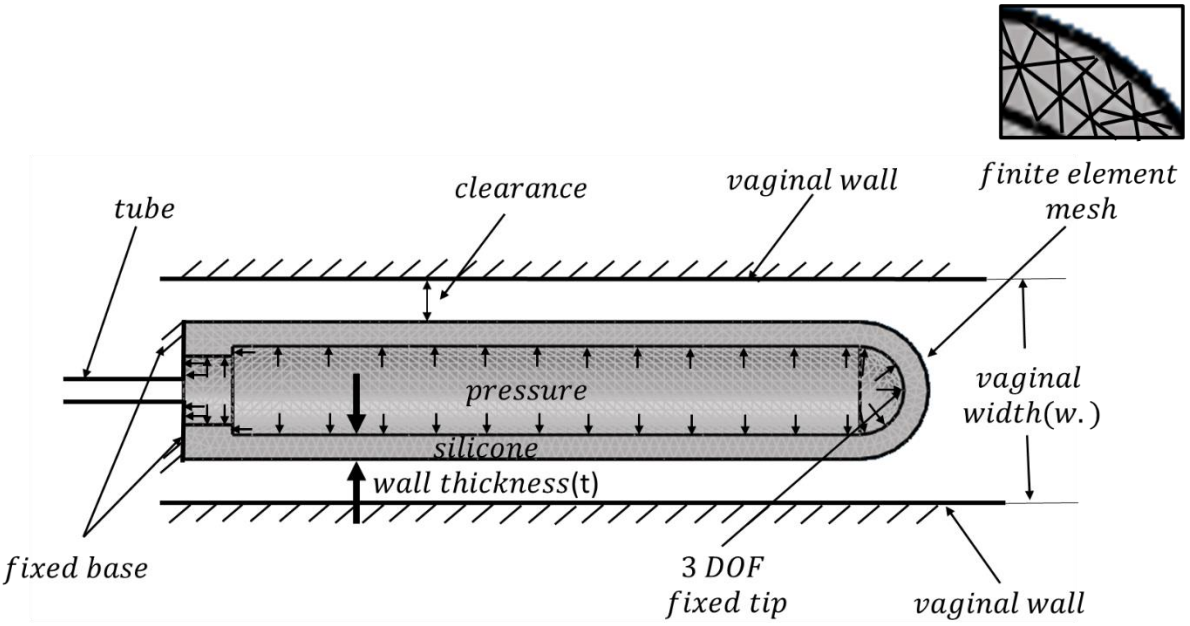

Figure 33: Schematic of vaginal dilator for finite element analysis [47]

4.2.2 Change of Cross-Section of the Dilator as a Function of Pressure

A finite element analysis was first conducted without the constraints of the rigid walls. The inflation of the dilator as a function of pressure was simulated while keeping all other dimensions and boundary conditions the same. The material was characterized by the Mooney-Rivlin parameter discussed in Chapter 3. For the silicone used, the Mooney-Rivlin coefficients were C_1= 0.026 MPa and C_2= 0.0093 MPa.

Figure 34 shows the side view of a typical dilator during inflation. We observe that the largest inflation exists at the center, while the least inflation occurs at the ends. Figure 35 shows the cross-sectional area of the dilator as a function of internal pressure for four different wall

thicknesses of silicone. We observe that the maximum area of the dilator decreases as the dilator wall thickness increases.

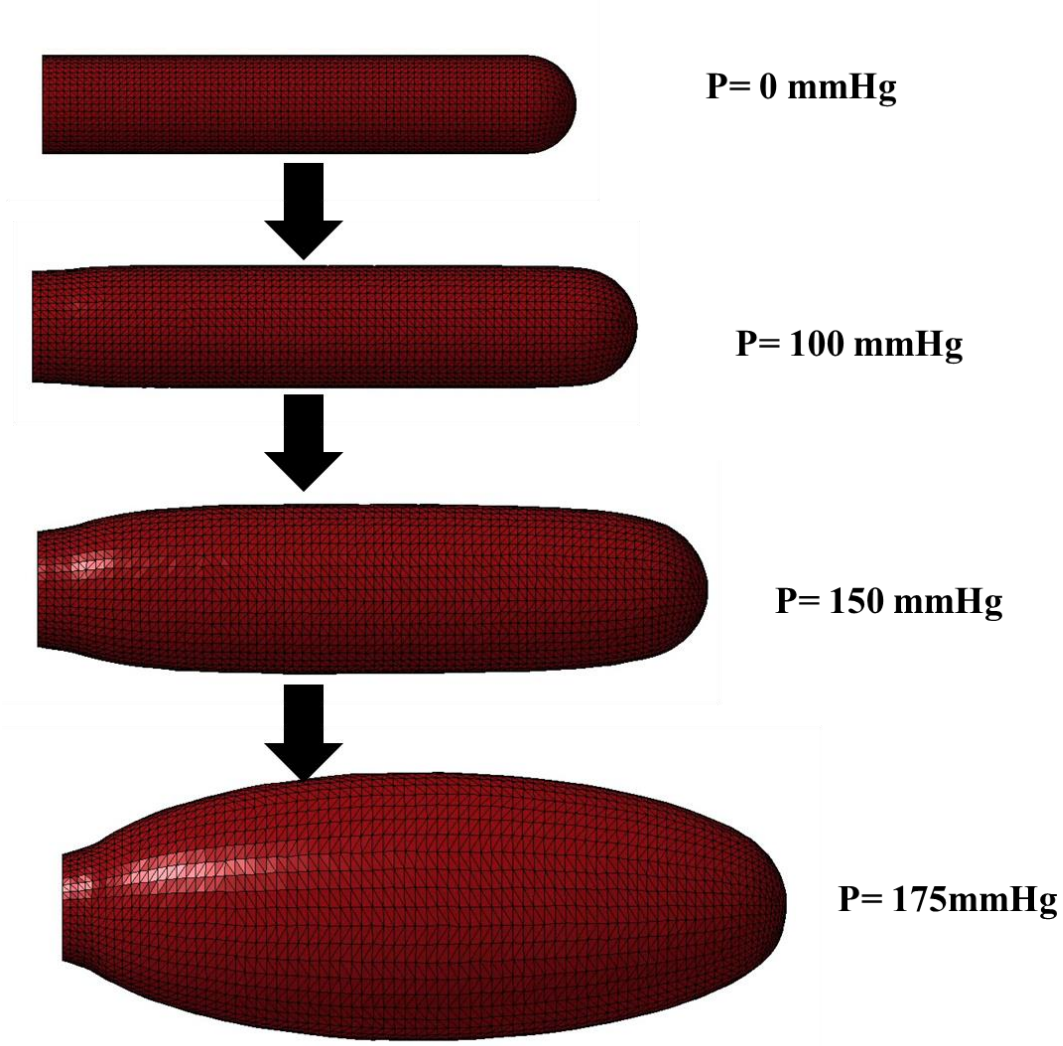

Figure 34: Cross-section of dilator (2mm wall thickness) before and after inflation using finite element simulation

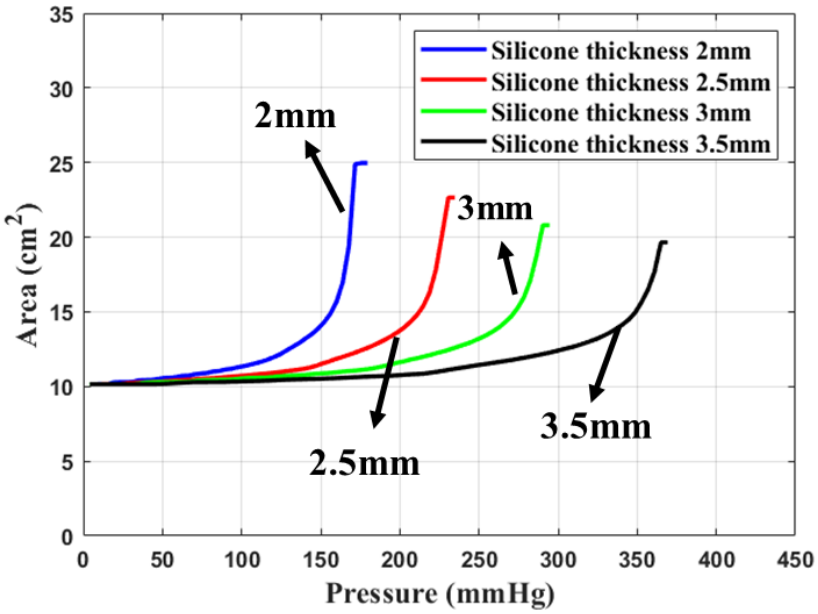

Figure 35: Cross-section area of dilator for four silicone wall thicknesses (2mm, 2.5mm, 3mm, 3.5mm) as a function of pressure

4.2.3 Force on the Vaginal Wall Dilator

Figure 36 shows the maximum force exerted by the dilator on the vaginal wall for the dilator wall thickness of 2mm, 2.5mm, 3mm, and 3.5mm dilator, respectively. We observe that that force exerted on the vaginal wall at constant pressure is larger for a small wall thickness than a large wall thickness.

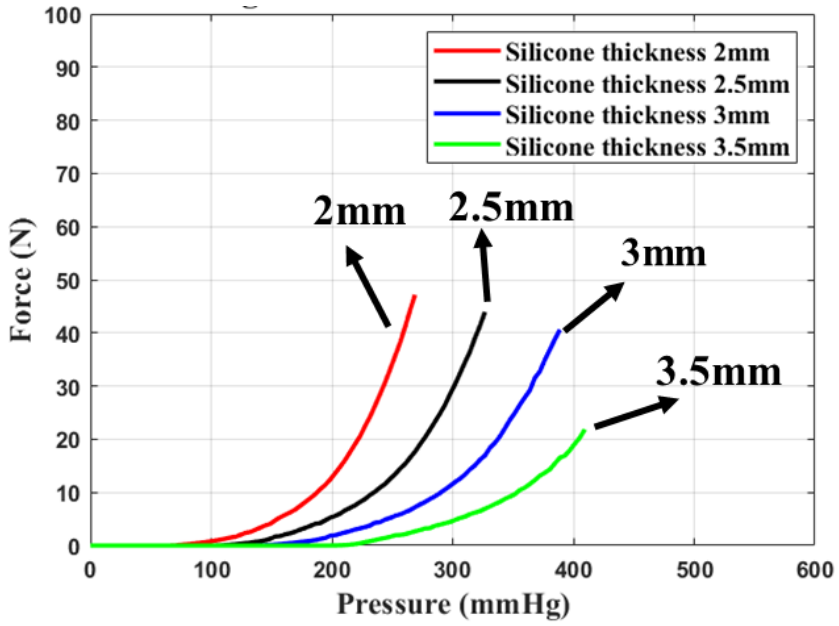

Figure 36: Force versus pressure for dilators with different wall thickness (2mm, 2.5mm, 3mm, 3.5mm) and 15mm vaginal wall distance

4.3 Stress Concentration at the Interface of the Dilator and the Plastic Air Tube

From our finite element simulation, we observe stress concentration at the junction part between the dilator and plastic tube. This stress concentration causes large deformation, which in turn leads to leakage problems of the dilator.

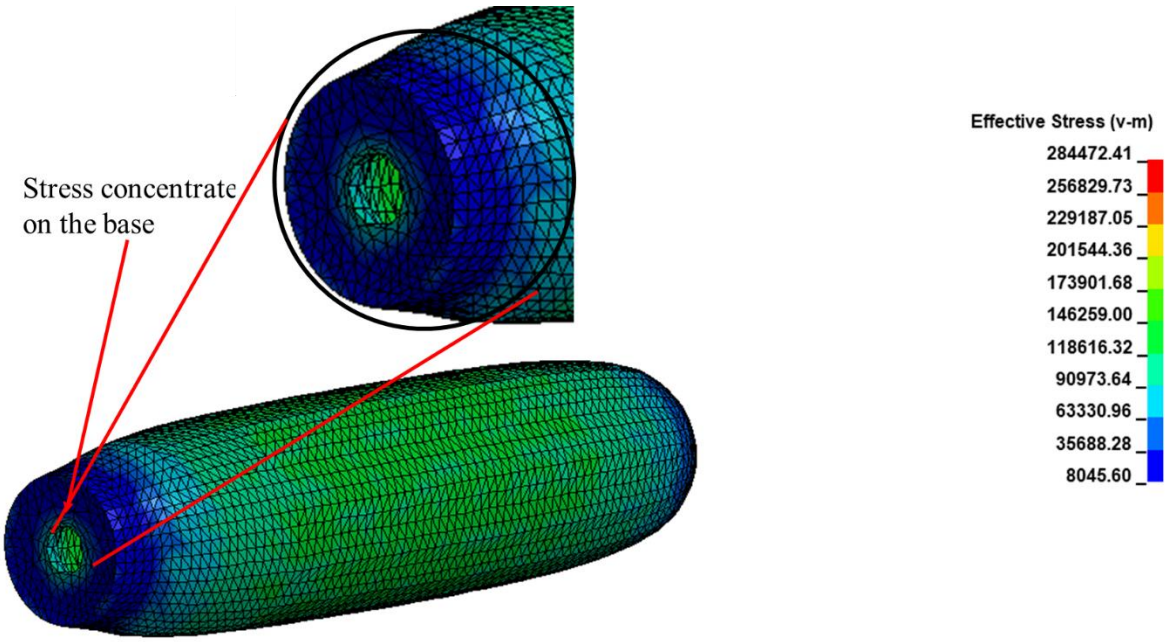

Figure 37: Stress concentration at the base of the dilator (wall thickness 2.5mm)

Chapter 2 and Chapter 4, in part, contains published material as it appears in Rafaela Simoes-Torigoe, Po-Han Chen, Yu M. Li, Matthew Kohanfars, Karcher Morris, Casey W. Williamson, Milan Makale, Jyoti Mayadev, Frank Talke, “Design and Validation of an Automated Dilator Prototype for the Treatment of Radiation Induced Vaginal Injury,” 2021 43rd Annual International Conference of the IEEE Engineering in Medicine & Biology Society (EMBC), IEEE. The thesis author was a co-author of this paper.

Chapter 5 Experimental Measurement of Dilator Inflation

5.1 Introduction

To investigate the inflation of the vaginal dilator we have measured the cross-sectional area of the dilator as a function of internal pressure and the force that the dilator exerts on the vaginal wall during inflation. Four wall thicknesses of dilators (2mm, 2.5mm, 3mm, and 3.5mm) were used and compared. These experiments were performed to allow comparison with results from the finite element analysis.

5.2 Experimental Setup

The first experiment was to measure the inflation of the dilator with a fixed volume of air injected into the dilator. The cross-sectional area of the dilator and the pressure inside the dilator chamber was recorded and compared to the finite element simulation.

Figure 38 shows the experimental setup for measuring the area and pressure of the vaginal dilator during inflation. The setup consists of a dilator, a camera, a black background, a peristaltic pump, a syringe pump, and a pressure sensor. A camera was used to record the dilator shape during inflation. The recorded video was used to calculate the area inflation of the dilator over time using MATLAB. A black background was used to improve the visibility of the dilator

image during inflation. A peristaltic pump was used to provide air for the dilator to expand, and a syringe pump was used to measure the volume of inflation. A pressure sensor was used to measure the pressure of air in the dilator.

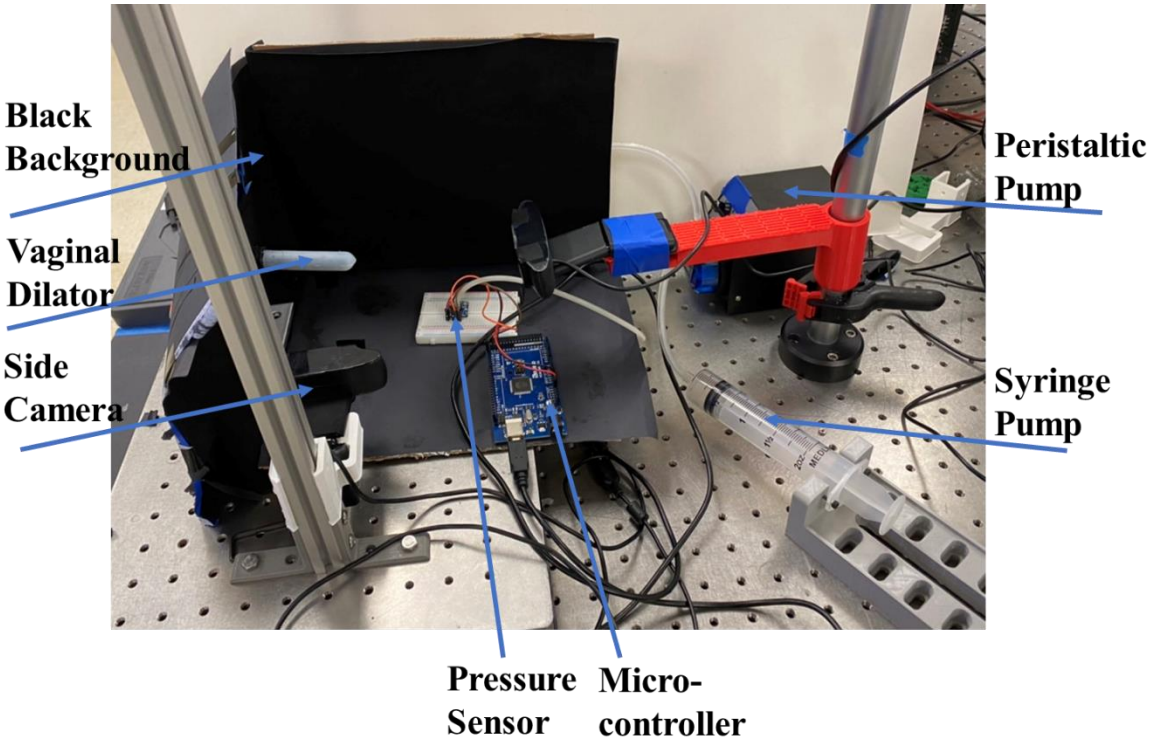

Figure 38: Experimental setup of cross-sectional area and pressure measurement

5.2.1 Dilator Pressure and Area Test Results

Four dilator wall thicknesses (2mm, 2.5mm, 3mm, and 3.5mm) were investigated. The dilators were inflated to a constant volume of 30ml. In Figure 39, we show the area increase as a function of pressure for a wall thickness before and after filtering of the pressure data. Figure 40 shows the results for four different wall thickness dilators after filtering.

Figure 40 shows the change in cross sectional area as a function of pressure for four values of wall thicknesses. We observe that the measurements agree well with the numerical simulation of section 4.2.2

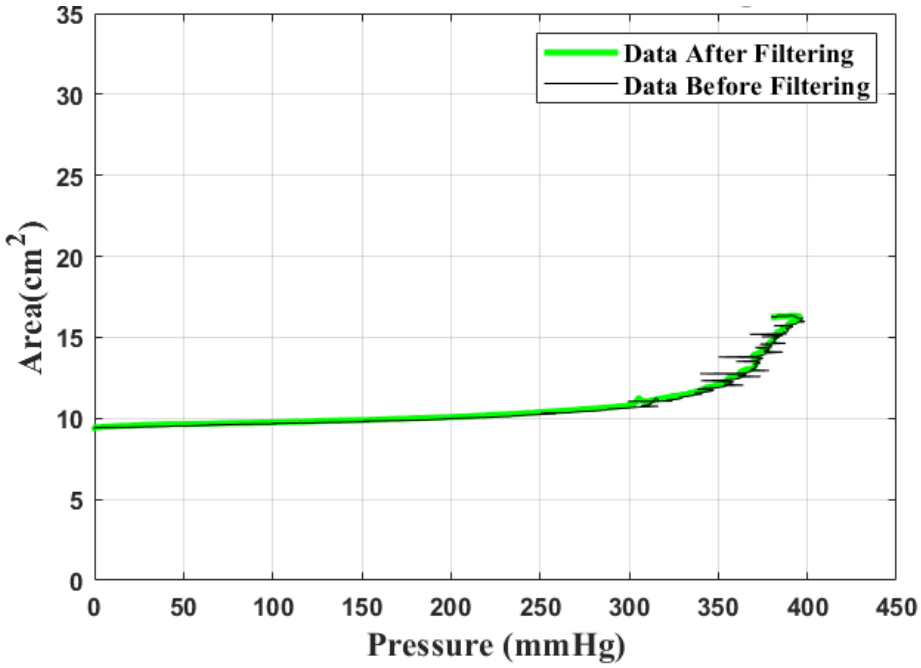

Figure 39: Area versus pressure for 3.5mm thick dilator

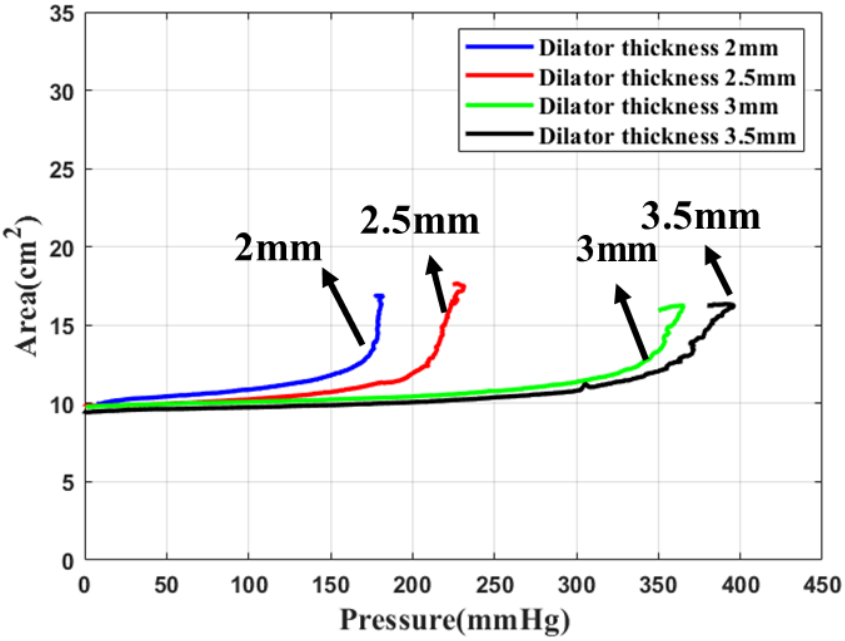

Figure 40: Area versus pressure for four different dilator wall thicknesses

From the experimental results, we observed that the cross-sectional area of the dilator was smaller than the prediction of the finite element simulation (Figure 35).

5.3 Experimental Setup of Measurement of Force and Pressure of the Dilator on the Vaginal Wall

Figure 41 shows the experimental setup for measuring the force and pressure of an inflating vaginal dilator against the vaginal wall. The distance between the vaginal walls was adjusted by an actuator arm controlled by a microcontroller to simulate different dimensions of the vaginal canal. A peristaltic pump was used to provide an adequate amount of air for the dilator to expand, and the syringe pump was used to measure the amount of volume of inflation. A pressure

sensor was used to measure the dilator pressure during inflation, while a load cell was used for measuring the force of the dilator against the vaginal wall. Four different dilator thicknesses were investigated, keeping the distance between the vaginal wall at 15mm.

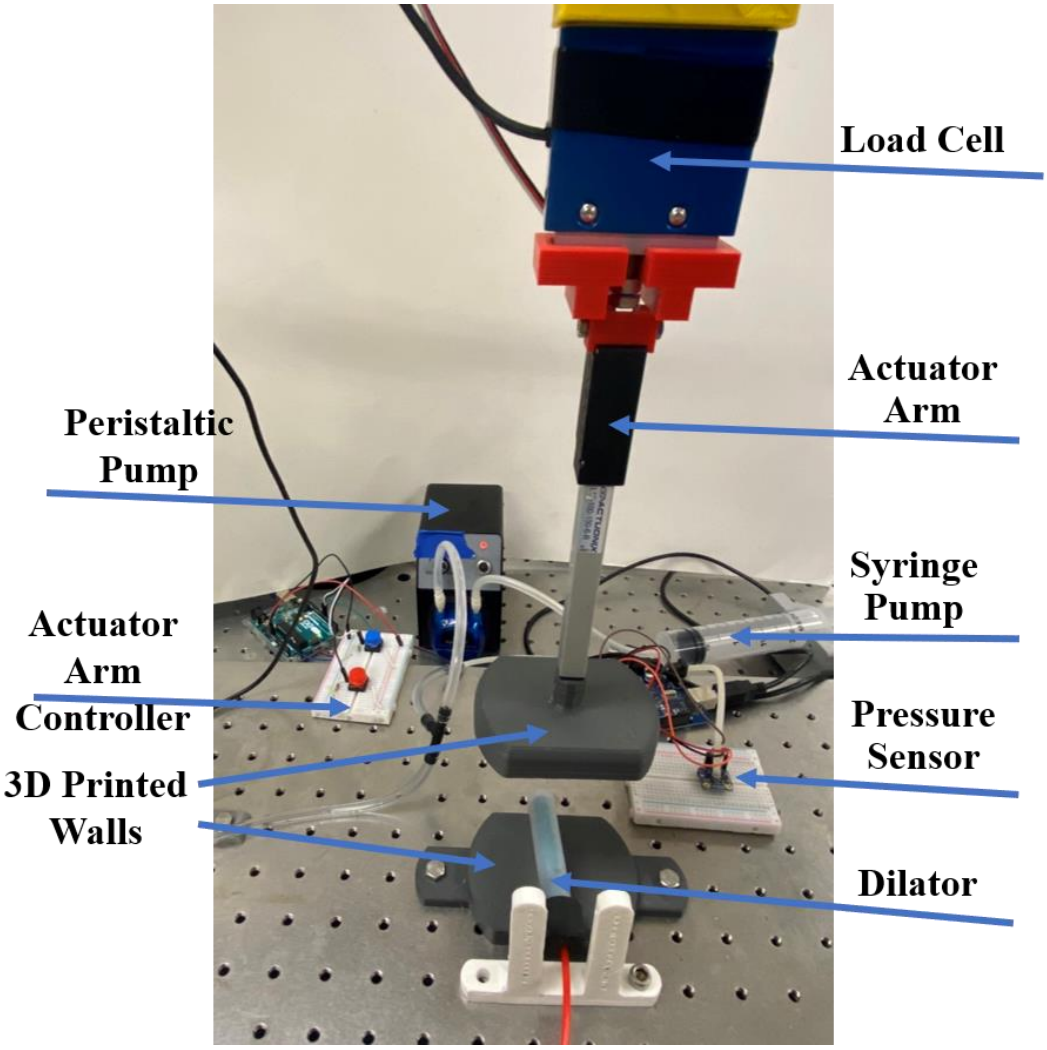

Figure 41: Experimental setup of force and pressure measurement

Figure 42 shows the average force of the vaginal wall for a dilator wall thickness of 2mm. The maximum standard deviation of the force was 4.63 N and the pressure was 33.61 mmHg. Figure 43 shows the average pressure and force of the inflating dilator against the vaginal wall.

From Figure 43, we observe that the maximum force increases as the dilator wall thickness decreases keeping the internal pressure constant.

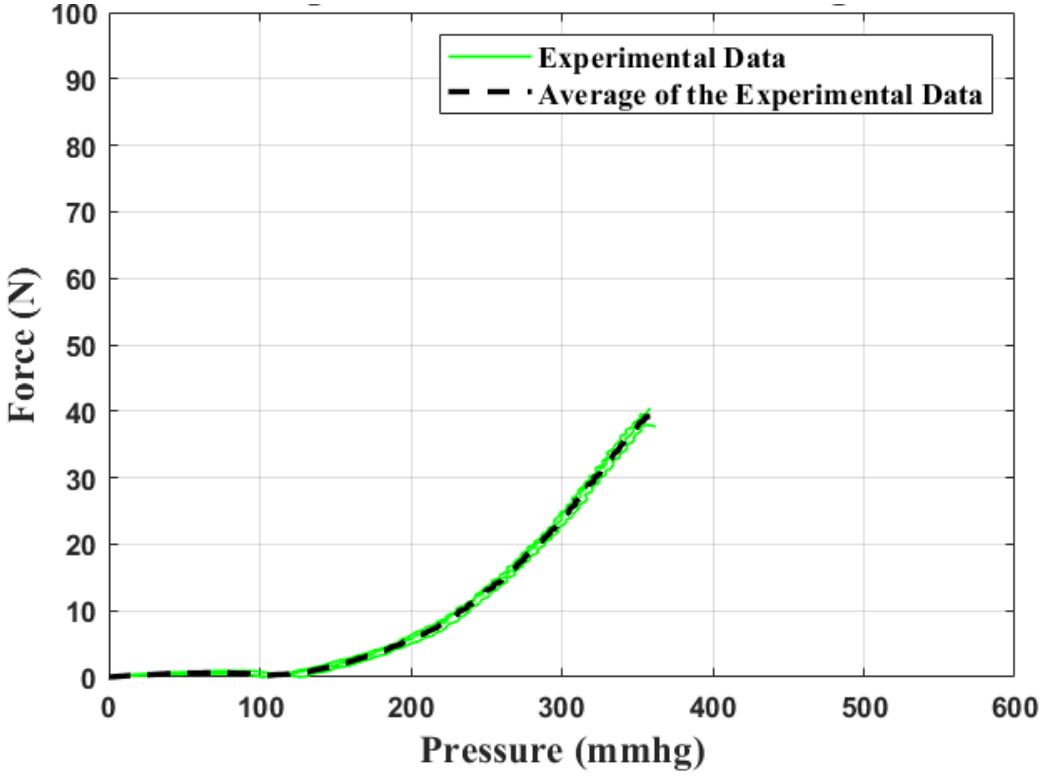

Figure 42: Force versus pressure for 2mm wall thickness and 15mm vaginal wall distance

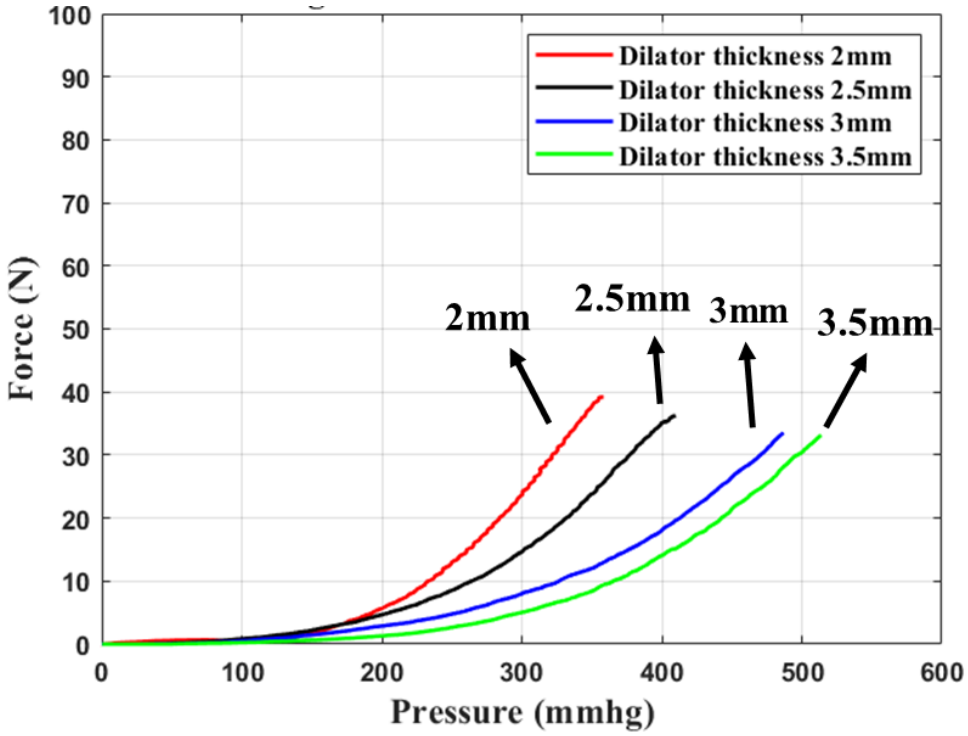

Figure 43: Force versus pressure for 15mm vaginal wall distance for four different wall thicknesses

The experimental measurements show a higher maximum pressure compared to the finite element simulation (Figure 36), but the trend is in good agreement between numerical calculation and experimental measurement. Differences in pressure between the experimental and analytical model were mainly due to the friction between the vaginal wall and the dilator in the experimental setup.

5.3.1 Discussion

From both the experimental studies and finite element simulation, it can be concluded that dilators with smaller wall thickness inflate easier than dilators with thicker wall thickness. On the other hand, the maximum pressure in a dilator with large wall thickness is larger than in a thin-walled dilator. Clearly, the experimental results and numerical studies show similar trends.

Chapter 6 Summary and Future Work

Vaginal stenosis (VS) is one of the common side effects of radiotherapy. To treat vaginal stenosis, a vaginal dilator is needed to promote epithelialization and increased vascularity of the tissues [8][12]. In this thesis, a vaginal dilator was investigated that can gradually be inflated. The dilator was made of commercially available silicone. Material characterization of silicone was conducted, and stress versus strain relationships for hyperelastic silicone was performed. In addition, finite element simulations and experiment measurements were carried out using inflatable vaginal dilators with several different wall thicknesses of silicone. The deformation of the dilator and the force of the dilator against the vaginal wall were measured.

Future work on the dilator prototype should focus on improving the dual chamber dilator approach. The manufacturing time and steps should be decreased and the reliability of the dual chamber dilator must be improved. Additional dilator chambers would be desirable to allow control of the inflation at specific locations of the vaginal canal. A more ergonomic dilator handle should be created to increase the convenience for the patient holding the dilator. Different kinds of materials should be explored for the dilator handle.

The monitoring system that inflates and records the information of the dilator should be more user-friendly, and the control system should focus on supplying both a “common therapy” mode for patients and a “maximum pressure test” mode. The design of the housing and reservoir should be improved to be more user-friendly, and the accuracy of the pressure and flow rate measurements should be improved.

Finite element analysis should be conducted before manufacturing new dilators. The simulation should predict how well the dilator expands when it is in contact with tissue. For this purpose, the design of a so-called vaginal phantom should be considered.

In our present studies**,** we simulated the dilator by it positioning it between two flat boundaries with adjustable distances to mimic different dimensions of the vaginal canal. In the future, silicone vaginal phantoms must be designed and implemented to study the interactions between the dilator and the vaginal tissue. The material stiffness of the phantom should be similar to the vaginal tissue to provide an accurate measurement of the force between dilator and phantom.

On the medical side, the project needs to gain Institutional Review Boards (IRB) approval, and patient testing in the clinic is needed.

After the inflatable vaginal dilator system is tested, it would be desirable to initiate commercialization of the dilator.

References

[1] Cohen, P. A., Jhingran, A., Oaknin, A., and Denny, L., 2019, "Cervical Cancer," The Lancet, 393(10167), pp. 169–182.

[2] Ahmed, S., Ahmed, R., Idris, S., and Sabitu, K., 2013, "Knowledge, Attitude and Practice of Cervical Cancer Screening among Market Women in Zaria, Nigeria," Niger Med J, 54(5), p. 316.

[3] Arbyn, M., Weiderpass, E., Bruni, L., de Sanjosé, S., Saraiya, M., Ferlay, J., and Bray, F., 2020, "Estimates of Incidence and Mortality of Cervical Cancer in 2018: A Worldwide Analysis," The Lancet Global Health, 8(2), pp. e191–e203.

[4] Hofsjö, A., 2018, Vaginal Morphological Changes in Cervical Cancer Survivors.

[5] Morris, L., Do, V., Chard, J., and Brand, A., 2017, "Radiation-Induced Vaginal Stenosis: Current Perspectives," IJWH, Volume 9, pp. 273–279.

[6] RadiologyInfo.org, "Brachytherapy" [Online]. Available: https://www.radiologyinfo.org/en/info/brachy. [Accessed: 02-Apr-2017].

[7] American Cancer Society, "Treating Endometrial Cancer," p. 34.

[8] Mirabeau-Beale, K., Hong, T. S., Niemierko, A., Ancukiewicz, M., Blaszkowsky, L. S., Crowley, E. M., Cusack, J. C., Drapek, L. C., Kovalchuk, N., Markowski, M., Napolitano, B., Nyamwanda, J., Ryan, D. P., Wolfgang, J., Kachnic, L. A., and Wo, J. Y., 2015, "Clinical and Treatment Factors Associated with Vaginal Stenosis after Definitive Chemoradiation for Anal Canal Cancer," Practical Radiation Oncology, 5(3), pp. e113–e118.

[9] Shield, P. W., 1995, "Chronic Radiation Effects: A Correlative Study of Smears and Biopsies from the Cervix and Vagina," Diagn. Cytopathol., 13(2), pp. 107–119.

[10] Varytė, G., and Bartkevičienė, D., 2021, "Pelvic Radiation Therapy Induced Vaginal Stenosis: A Review of Current Modalities and Recent Treatment Advances," Medicina, 57(4), p. 336.

[11] Liu, M., Juravic, M., Mazza, G., and Krychman, M. L., 2021, "Vaginal Dilators: Issues and Answers," Sexual Medicine Reviews, 9(2), pp. 212–220.

[12] Hartman, P., and Diddle, A. W., 1972, "Vaginal Stenosis Following Irradiation Therapy for Carcinoma of the Cervix Uteri," Cancer, 30(2), pp. 426–429.

[13] Miles, K., and Miles, S., 2021, "Low Dose, High Frequency Movement Based Dilator Therapy for Dyspareunia: Retrospective Analysis of 26 Cases," Sexual Medicine, 9(3), p. 100344.

[14] Macey, K., Gregory, A., Nunns, D., and das Nair, R., 2015, "Women's Experiences of Using Vaginal Trainers (Dilators) to Treat Vaginal Penetration Difficulties Diagnosed as Vaginismus: A Qualitative Interview Study," BMC Women's Health, 15(1), p. 49.

[15] Law, E., Kelvin, J. F., Thom, B., Riedel, E., Tom, A., Carter, J., Alektiar, K. M., and Goodman, K. A., 2015, “Prospective Study of Vaginal Dilator Use Adherence and Efficacy Following Radiotherapy,” Radiotherapy and Oncology, 116(1), pp. 149–155.

[16] Smooth-On, “Durometer Shore Hardness Scale” [Online]. Available: https://www.smooth-on.com/page/durometer-shore-hardness-scale/.

[17] prasanthinidamarthy, 2021, “Elasticity and Plasticity” [Online]. Available: https://www.geeksforgeeks.org/elasticity-and-plasticity/.

[18] minaprem.com, “Difference Between Elasticity and Plasticity,” Difference Between Elasticity and Plasticity [Online]. Available: http://www.difference.minaprem.com/solid/difference-between-elasticity-and-plasticity/.

[19] Martins, P. A. L. S., Natal Jorge, R. M., and Ferreira, A. J. M., 2006, “A Comparative Study of Several Material Models for Prediction of Hyperelastic Properties: Application to Silicone-Rubber and Soft Tissues,” Strain, 42(3), pp. 135–147.

[20] Yeoh, O. H., 1997, "Hyperelastic material models for finite element analysis of rubber." Journal of Natural Rubber Research, 12(1997), pp.142-153.

[21] Yang, L. M., Shim, V. P. W., and Lim, C. T., 2000, “A Visco-Hyperelastic Approach to Modelling the Constitutive Behaviour of Rubber,” International Journal of Impact Engineering, 24(6–7), pp. 545–560.

[22] Pinsky, P. M., Ortiz, M., and Pister, K. S., 1983, “Numerical Integration of Rate Constitutive Equations in Finite Deformation Analysis,” Computer Methods in Applied Mechanics and Engineering, 40(2), pp. 137–158.

[23] TWI, 2022, “WHAT IS FINITE ELEMENT ANALYSIS (FEA)?” [Online]. Available: https://www.twi-global.com/technical-knowledge/faqs/finite-element-analysis.

[24] IEEE Innovation at Work, “The Advantages of the Finite Element Method” [Online]. Available: https://innovationatwork.ieee.org/the-advantages-of-fem/.

[25] Beth, S., 2005, “Complete Vaginismus Treatment Kit,” Journal of Women’s Health Physical Therapy, 29(3), p. 74.

[26] Juravuc, M., 2021, “SYSTEMS AND METHODS FOR THE TREATMENT AND PREVENTION OF FEMALE PELVIC DYSFUNCTION,”

[27] Adamson, C. D., Naik, B. J., and Lynch, D. J., 2004, “The Vacuum Expandable Condom Mold: A Simple Vaginal Stent for McIndoe-Style Vaginoplasty:,” Plastic and Reconstructive Surgery, 113(2), pp. 664–666.

[28] Visakh, P. M., Thomas, S., Chandra, A. K., and Mathew, Aji. P., eds., 2013, Advances in Elastomers I: Blends and Interpenetrating Networks, Springer Berlin Heidelberg, Berlin, Heidelberg.

[29] Nwankire, C. E., Ardhaoui, M., and Dowling, D. P., 2009, “The Effect of Plasma-Polymerised Silicon Hydride-Rich Polyhydrogenmethylsiloxane on the Adhesion of Silicone Elastomers: Effect of Plasma-Polymerised PHMS on Adhesion of Silicone Elastomers,” Polym. Int., 58(9), pp. 996–1001.

[30] Carpenter, J. C., Cella, J. A., and Dorn, S. B., 1995, "Study of the Degradation of Polydimethylsiloxanes on Soil," Environ. Sci. Technol., 29(4), pp. 864–868.

[31] Mazurek, P., Vudayagiri, S., and Skov, A. L., 2019, "How to Tailor Flexible Silicone Elastomers with Mechanical Integrity: A Tutorial Review," Chem. Soc. Rev., 48(6), pp. 1448–1464.

[32] Studer, J., 2019, "Material Q&A: Elastomer and Plastic Materials" [Online]. Available: https://www.valvemagazine.com/articles/elastomer-and-plastic-materials.

[33] Marckmann, G., and Verron, E., 2006, "Comparison of Hyperelastic Models for Rubber-Like Materials," Rubber Chemistry and Technology, 79(5), pp. 835–858.

[34] Wex, C., Arndt, S., Stoll, A., Bruns, C., and Kupriyanova, Y., 2015, "Isotropic Incompressible Hyperelastic Models for Modelling the Mechanical Behaviour of Biological Tissues: A Review," Biomedical Engineering / Biomedizinische Technik, 60(6).

[35] Mooney, M., 1940, "A Theory of Large Elastic Deformation," Journal of Applied Physics, 11(9), pp. 582–592.

[36] Jadhav, A. N., Bahulikar, S., and Sapate, N. H., 2016, "Comparative Study of Variation of Mooney-Rivlin Hyperelastic Material Models under Uniaxial Tensile Loading," International Journal of Advance Research and Innovative Ideas in Education, 2(4), pp. 212–216.

[37] Morris, K., 2021, "Design of an Esophageal Deflection and Thermal Monitoring Device for Use during Cardiac Ablation Procedures," UC San Diego Electronic Theses and Dissertations, UC San Diego.

[38] Gopesh, T., and Friend, J., 2021, "Facile Analytical Extraction of the Hyperelastic Constants for the Two-Parameter Mooney–Rivlin Model from Experiments on Soft Polymers," Soft Robotics, 8(4), pp. 365–370.

[39] Di Lecce, M., Onaizah, O., Lloyd, P., Chandler, J. H., and Valdastri, P., 2022, "Evolutionary Inverse Material Identification: Bespoke Characterization of Soft Materials Using a Metaheuristic Algorithm," Front. Robot. AI, 8, p. 790571.

[40] Apinsathanon, P., Bhattarai, B. P., Suphangul, S., Wongsirichat, N., and Aimjirakul, N., 2021, "Penetration and Tensile Strength of Various Impression Materials of Vinylsiloxanether, Polyether, and Polyvinylsiloxane Impression Materials," Eur J Dent, p. s-0041-1735793.

[41] Marechal, L., Balland, P., Lindenroth, L., Petrou, F., Kontovounisios, C., and Bello, F., 2021, "Toward a Common Framework and Database of Materials for Soft Robotics," Soft Robotics, 8(3), pp. 284–297.

[42] ELKEM, 2019, "SILBIONE RTV 4410 1/1 A&B."

[43] SIMSCALE, 2021, "What Is FEA | Finite Element Analysis?" [Online]. Available: https://www.simscale.com/docs/simwiki/fea-finite-element-analysis/what-is-fea-finite-element-analysis/.

[44] Harish, A., 2020, "Finite Element Method – What Is It? FEM and FEA Explained," SIMSCALE [Online]. Available: https://www.simscale.com/blog/2016/10/what-is-finite-element-method/.

[45] English, T., 2019, “What Is Finite Element Analysis and How Does It Work?” Interesting Engineering [Online]. Available: https://interestingengineering.com/what-is-finite-element-analysis-and-how-does-it-work.

[46] Sadiku, M. N. O., 1989, “A Simple Introduction to Finite Element Analysis of Electromagnetic Problems,” IEEE Trans. Educ., 32(2), pp. 85–93.

[47] Simoes-Torigoe, R., Chen, P.-H., Li, Y. M., Kohanfars, M., Morris, K., Williamson, C. W., Makale, M., Mayadev, J., and Talke, F., 2021, “Design and Validation of an Automated Dilator Prototype for the Treatment of Radiation Induced Vaginal Injury,” 2021 43rd Annual International Conference of the IEEE Engineering in Medicine & Biology Society (EMBC), IEEE, Mexico, pp. 1562–1565.

[48] Brand, A. H., Bull, C. A., and Cakir, B., 2006, “Vaginal Stenosis in Patients Treated with Radiotherapy for Carcinoma of the Cervix,” Int J Gynecol Cancer, 16(1), p. 288.

[49] Global Cancer Observatory, 2022, “Worldwide Cancer Data,” World Cancer Research Fund International [Online]. Available: https://www.wcrf.org/cancer-trends/worldwide-cancer-data/.

[50] Simoes Torigoe, R., 2022, “Development of a Model to Simulate Radiation Induced Vaginal Stenosis,” University of California San Diego.

[51] 안진수, “What Is the Difference between a Hyperelastic Material and an Elastic Material in RecurDyn?,” FunctionBay Tech support [Online]. Available: https://support.functionbay.com/en/faq/single/87/difference-hyperelastic-material-elastic-material-recurdyn.

[52] Lumencandela, “Elasticity and Plasticity,” OER services, University Physics Volume 1 [Online]. Available: https://courses.lumenlearning.com/suny-osuniversityphysics/chapter/12-4-elasticity-and-plasticity/.

[53] SIMSCALE, “Hyperelastic Materials” [Online]. Available: https://www.simscale.com/docs/simulation-setup/materials/hyperelastic-materials/.

[54] Risangud, N., 2017, “Synthesis and Application of New Polymers for Agriculture : Pesticide Formulation,” Thesis or Dissertation (PhD), University of Warwick.

[55] “PRINCIPLES OF CONDENSATION POLYMERIZATION,” Crow [Online]. Available: https://polymerdatabase.com/polymer%20chemistry/Condensation%20Polymerization.html.

[56] “Free Radical Polymerization,” BYJU’S [Online]. Available: https://byjus.com/chemistry/free-radical-polymerization/.

[57] “Silicones,” BYJU’S [Online]. Available: https://byjus.com/jee/silicones/.

[58] Ohayon, J., Ambrosi, D., and Martiel, J.-L., 2017, “Hyperelastic Models for Contractile Tissues,” Biomechanics of Living Organs, Elsevier, pp. 31–58.

[59] Lai, W. M., Rubin, D., and Krempl, E., 2010, “The Elastic Solid,” Introduction to Continuum Mechanics, Elsevier, pp. 201–352.

[60] Bergström, J., 2015, “Elasticity/Hyperelasticity,” Mechanics of Solid Polymers, Elsevier, pp. 209–307.

[61] “MOONEY-RIVLIN MODEL,” Crow (polymerdatabase.com) [Online]. Available: http://polymerdatabase.com/polymer%20physics/Mooney-Rivlin%20Model.html.

[62] Hu, S., Morris, K., Chen, P.-H., Simoes-torigoe, R., Li, Y. M., Mayadev, J., and Talke, F. E., 2022, “A SOFT ROBOTIC CLOSED-LOOP SYSTEM FOR THE TREATMENT OF VAGINAL STENOSIS,”, 2022 JSME-IIP/ASME-ISPS Joint International Conference on Micromechatronics for Information and Precision Equipment (MIPE2022), August 28-31, 2022, Toyoda Auditorium of Nagoya University, Nagoya, Japan (Accepted)